



Norwegian
Meteorological
Institute

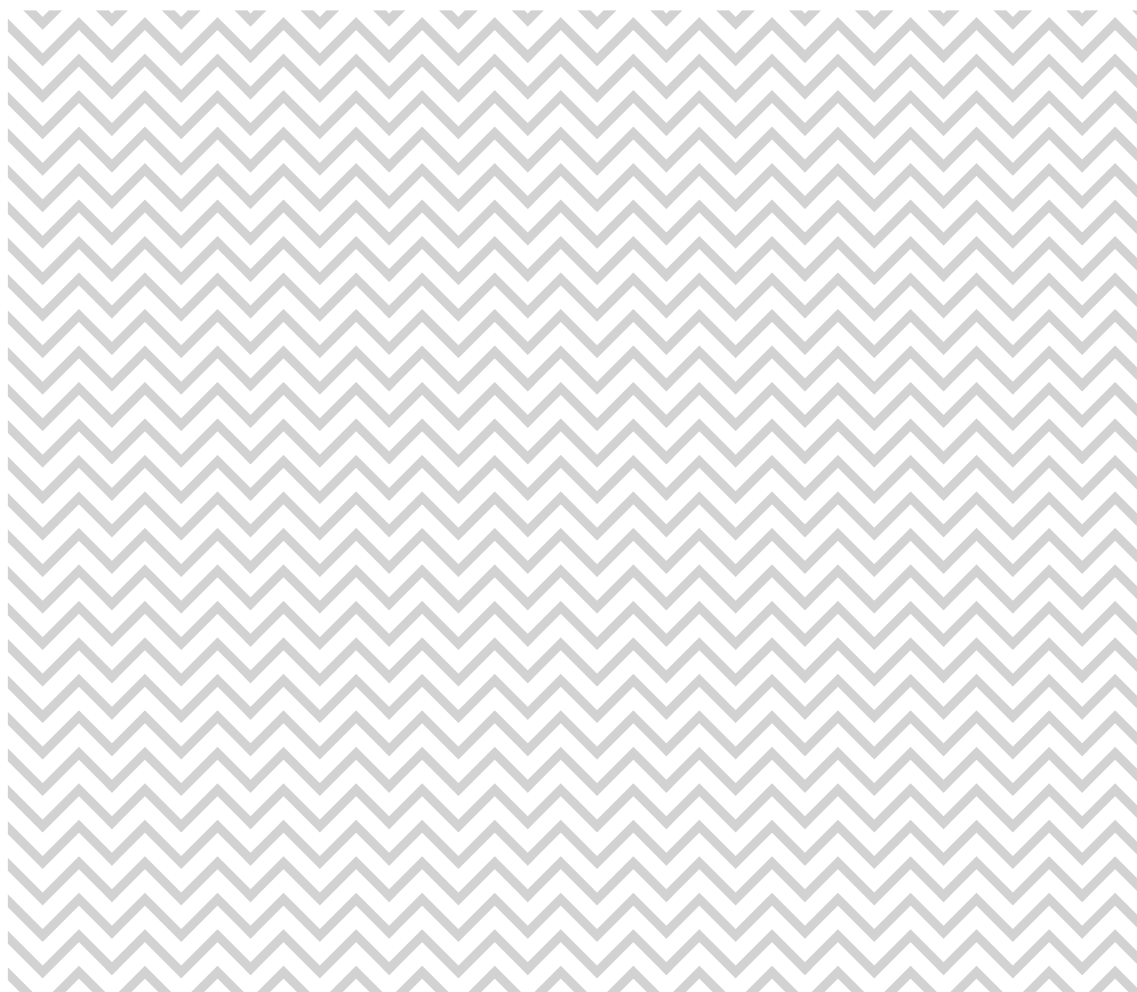
METreport

No. 16/2021
ISSN 2387-4201

Modelling of phyto-toxic ozone doses for Norway

– based on chemical data assimilation

David Simpson, Arjo Segers, Alvaro Valdebenito and Hilde Fagerli



M-2251 I 2022



Norwegian
Meteorological
Institute

METreport

Title Modelling of phyto-toxic ozone doses for Norway – based on chemical data assimilation	Date December 2, 2021
Section	Report no. 16/2021
Author(s) David Simpson, Arjo Segers, Alvaro Valdebenito and Hilde Fagerli Author name	Classification <input checked="" type="radio"/> Free <input type="radio"/> Restricted
Client(s) Norwegian Environment Agency	Client's reference
Abstract Phyto-toxic ozone dose (POD) is a term used to describe the uptake of the harmful gas ozone into the stomata of plants. In this project we have used a version of the EMEP MSC-W chemical transport model which assimilates observational data of ozone and other compounds. The model results suggest that critical levels for deciduous forests are exceeded across essentially all of Norway in both 2018 and 2019, and exceedance was also widespread coniferous forests. Exceedances for other semi-natural vegetation and crops were also found in southern and eastern parts of Norway, especially in 2018. Although there are many uncertain aspects of such POD calculations, this study has demonstrated that the use of data assimilation leads to much improved model estimates of ozone and a related metric (AOT40), and thus provides a good basis for modelling POD across Norway. Future work would include refinements in the assimilation techniques, but more importantly more detailed characterisation of the vegetation characteristics in this region.	
Keywords Ozone, modelling, POD, vegetation	

H Fagerli

Disciplinary signature

2

Lars-Anders Bræin

Responsible signature

SUMMARY

Phyto-toxic ozone dose (POD) is a term used to describe the uptake of the harmful gas ozone into the stomata of plants. POD-values over a certain threshold, Y , have been shown to cause reductions in biomass of crops and semi-natural vegetation. In this project we have used a version of the EMEP MSC-W chemical transport model which assimilates observational data of ozone and other compounds using a 3D Var assimilation system. We show that the use of 3D-Var assimilation leads to markedly better reproduction of the daily ozone concentrations, and of the AOT40 metric (EU definition), at the Nordic sites.

We have calculated POD for four classes of vegetation: deciduous and coniferous forests, (other) seminatural vegetation, and crops. The critical levels (CLs) for deciduous forests were exceeded across essentially all of Norway in both 2018 and 2019, with values often exceeding three times the CL in south-eastern areas. Exceedances are higher in 2018, consistent with the exceptionally warm and sunny summer of that year. For coniferous forests exceedance of the CL was also widespread. Exceedance of the CL for IAM_SNL occurs mainly in south eastern Norway. For crops exceedances were seen along the southern and eastern coastal areas in both years, with larger exceedances in 2018. Although this study does not aim to a proper estimate of yield loss for crops in Norway, the modelled POD values suggest that losses of the order of 10% can occur in south-eastern coastal areas of Norway.

Although there are many uncertain aspects of such POD calculations, this study has demonstrated that the use of 3-D Var leads to much improved model estimates of ozone and AOT40, and thus provides a good basis for modelling POD across Norway. Future work would include refinements in the assimilation techniques, but more importantly more detailed characterisation of the vegetation characteristics in this region.

Contents

1	Introduction	5
1.1	Ozone metrics	5
1.2	POD metrics	6
1.3	AOT40	7
1.4	Quantification of risk	8
2	Methods	11
2.1	The EMEP MSC-W chemical transport model	11
2.2	Data assimilation system	12
2.3	Measurements used	13
3	Model evaluation	16
3.1	Daily maximum ozone concentrations	16
3.2	AOT40	18
4	Modelled POD values	21
4.1	Deciduous forests	21
4.2	Coniferous forests	21
4.3	Semi-natural vegetation	23
4.4	Crops	26
4.5	AOT40 metrics?	28
5	Discussion and Conclusions	28
S1	Model evaluation - daily maximum ozone	S4
S2	Impacts on AOT40 metrics	S13
S3	Other activities	S15
S3.1	Experiments with zoom over Scandinavia	S15
S3.2	Topographic correction	S15

1 Introduction

Phyto-toxic ozone dose (POD) is a term used to describe the uptake of the harmful gas ozone into the stomata of plants. POD-values over a certain threshold, Y , have been shown to cause reductions in biomass of crops and semi-natural vegetation (*Emberson et al.*, 2001; *Pleijel et al.*, 2007; *Karlsson et al.*, 2007, 2009; *Mills et al.*, 2011a,b, 2018a,b; *Emberson*, 2020). In this project we have adapted the EMEP MSC-W chemical transport model so that it assimilates observational data of ozone and other compounds using a 3D Var assimilation system. This assimilation system adjusts the modelled O_3 in three dimensions, in order to provide fields of ozone which better match the observations. The assimilated ozone concentrations are used within the EMEP model to calculate POD values for different land-cover types. The approach used is similar to that of *Langner et al.* (2019), who estimated POD values over Sweden for 2013–2017, though the model used and the assimilation procedure were different.

This report documents the work, presents model evaluation with and without assimilation, and also presents maps of POD calculated for different ecosystems.

1.1 Ozone metrics

Ozone causes damage to crops only after it has been taken up via the stomata. Methods to assess flux-based metrics and associated dose-response relationships to estimate damage have been developed over many years within the Air Convention (*Emberson et al.*, 2000a, 2001; *Pleijel et al.*, 2007; *Mills et al.*, 2011a,b, 2018a), with the latest recommendations given in the Modelling and Mapping Manual (*UNECE*, 2017) – hereafter known just as the ‘Mapping Manual’, or simply the ‘MM’. The Mapping Manual provides information on the critical levels of a number of air pollutants for vegetation and the methodology for calculating critical level exceedances. For ozone (O_3), two types of critical levels are described for crops, forest trees and (semi-) natural vegetation: cumulative stomatal flux-based and cumulative concentration-based critical levels. Calculation of both incorporates the concept that the effects of O_3 are cumulative and values are summed over a specific threshold flux or concentration during daylight hours for a defined time period. According to the Mapping Manual, cumulative stomatal O_3 fluxes are considered biologically more relevant as they provide an estimate of the amount of O_3 entering the leaf pores and causing damage inside the plant.

1.2 POD metrics

The metric which is suggested for cumulative stomatal O₃ fluxes is the phyto-toxic ozone dose (POD_Y), which is the accumulated stomatal ozone flux over a threshold Y, i.e.:

$$\text{POD}_Y = \int \max(F_{st} - Y, 0) dt \quad (1)$$

where stomatal flux F_{st} , and threshold, Y , are in nmole O₃ m⁻² (PLA) s⁻¹. This integral is evaluated over time, from the start of the growing season (SGS), to the end (EGS). The Mapping Manual defined two specific categories of POD metrics:

1. POD_YSPEC– is a species or group of species-specific POD_Y that requires comprehensive input data and is suitable for detailed risk assessment.
2. POD_YIAM– is a vegetation-type specific POD_Y that requires less input data and is suitable for large-scale modelling, including integrated assessment modelling (IAM).

The POD_YIAM type metric was designed for use by models such as the EMEP CTM, in order to give an indicative risk assessment, and recognises that it is very difficult to specify the vegetation characteristics in detail for specific species across Europe. Accurate estimation of species-specific metrics with high Y thresholds, e.g. POD₆-SPEC for wheat is usually conducted with site-specific meteorological and ozone data.

The generic IAM species are implemented in the EMEP model as tiny fractions of all grid squares where vegetation is present. This procedure provides maps which cover all vegetated areas of Europe regardless of the real species distribution. Figure 1 illustrates the difference for deciduous forest. The left-hand map shows the raw EMEP model ‘IAM_DF’ results, whereas the right-hand map is masked to show only areas where the EMEP land-cover map has deciduous forest. It is clear that the raw ‘IAM_DF’ map provides calculations in many grid-cells where no such vegetation is thought to exist. The masked data show a much more realistic spatial distribution, but there are likely grid-cells where deciduous forests exist in reality (e.g. along the eastern coast of Norway), but where none are indicated by this map.

In this report we will evaluate POD metrics for three classes of generic IAM vegetation plus one species-specific:

IAM_WH	generic temperate/boreal crop, but largely based upon wheat
IAM_DF	broadleaf deciduous trees, based upon beech and birch in temperate/boreal regions
IAM_SNL	sensitive species in temperate grasslands
CF	coniferous forest, based upon Norway spruce

It should be noted that the parameters for CF in the EMEP model differ somewhat from those of the MM. For example, EMEP has a maximum stomatal conductance of $140 \text{ nmole O}_3 \text{ m}^{-2} \text{ (PLA) s}^{-1}$ (or $112 \text{ nmole O}_3 \text{ m}^{-2} \text{ (PLA) s}^{-1}$ after a phenology correction is applied), whereas the MM has $125 \text{ nmole O}_3 \text{ m}^{-2} \text{ (PLA) s}^{-1}$ for boreal forests, and $130 \text{ nmole O}_3 \text{ m}^{-2} \text{ (PLA) s}^{-1}$ for continental. The temperature of optimum stomatal conductance in EMEP is 18°C , but in the MM the boreal Norway spruce have 20°C . (Continental Norway spruce have 14°C in the MM, which is an indication of the uncertainties in these parameters.)

The Mapping Manual also defined critical level (CL) values for the different vegetation categories, plus a so-called ‘Ref10POD_Y’ value. The Ref10POD_Y value represents the POD_Y that would have been present in the pre-industrial atmosphere (with 10 ppb O₃), and is used as a base when setting the critical levels, as illustrated in Fig. 2. Table 1 summarises these for the vegetation classes we will present.

1.3 AOT40

The MM also details AOT40 (accumulated ozone over 40 ppb) as a concentration-based metric. However, the MM AOT40 requires calculation of the differences in O₃ concentrations between the measurement (or model) height and the top of the vegetation canopy, a task which makes this metric almost as difficult to calculate as POD_Y. In addition, these canopy-top O₃ concentrations cannot easily be verified. In this report we will provide model-measurement comparisons of AOT40 where the EU definition (EU, 2008) is used:

- AOT40f - forests, April-September, 08:00 – 19:59 CET
- AOT40c - crops, May–July, 08:00 – 19:59 CET

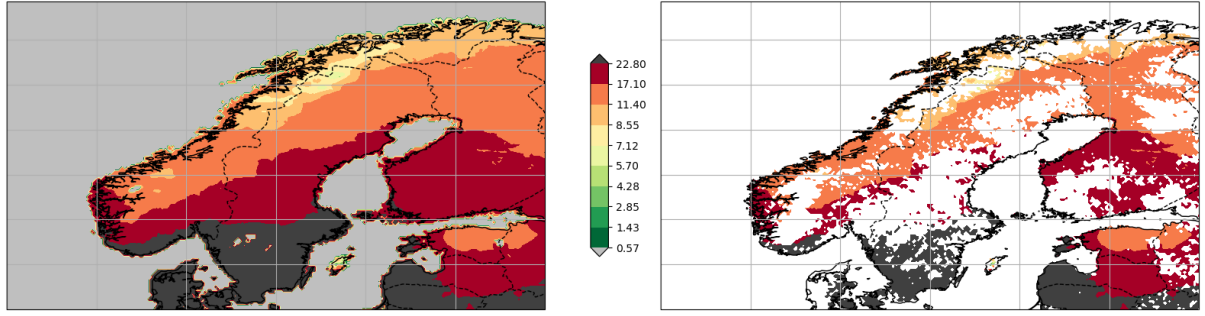


Figure 1: Illustration of the IAM approach for deciduous forests. The left-hand map shows the raw EMEP model output for POD_1IAM_DF (with assimilation) for 2018. The right-hand map shows the same data, but masked to show only areas where the EMEP model's land-cover map has deciduous forests. The contour levels reflect the critical levels (CL), which is $5.7 \text{ mmole O}_3 \text{ m}^{-2}$ (PLA), where PLA means projected leaf area. Contours span from 10% of the CL to $4 \times CL$ for IAM_DF.

The EU AOT40 metrics are intended for use with observed O_3 concentrations, without the additional step of calculating canopy-top O_3 . This makes this metric useful for comparison of modelled versus observed ozone – see Sect. 3. It should be noted though that AOT40 metrics are not very robust over Norway - the ambient O_3 concentrations often lie below or close to the 40 ppb threshold, making the estimates very sensitive to even small uncertainties in the estimated O_3 (Sofiev and Tuovinen, 2001; Tuovinen, 2000).

1.4 Quantification of risk

As defined in the Mapping Manual, if the calculated POD_Y is greater than the critical level (CL) for O_3 , exceedance of the critical level ($CL_{\text{exceedance}}$) is calculated as:

$$CL_{\text{exceedance}} = POD_Y - CL \quad (2)$$

For crops, the percentage yield loss (ΔY , %) is calculated following the dose response relationship between POD_3IAM_Crops and percentage reduction in wheat yield:

$$\Delta Y = (POD_3IAM_Crops - Ref10POD_Y) \times 0.64 \quad (3)$$

where $Ref10POD_Y$ represents a reference value corresponding to 10 ppb O_3 (Sect. 1.2, c.f Fig. 2), and 0.64 is the slope of the dose-response curve. According to the MM, the above approach can only be applied for crops, not for forest trees or other (semi-) natural

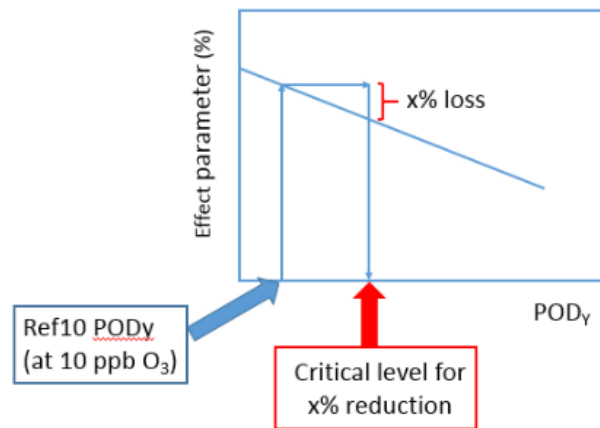


Figure 2: Method for using Ref10POD_Y (i.e. POD_Y at 10 ppb constant O₃) as reference point for O₃ critical level derivation. From *UNECE* (2017).

vegetation. For forest trees any such analysis is complicated by the fact the dose-response data are derived mainly from very young trees, and also that trees undergo many years of growth and ozone exposure. For semi-natural vegetation the impacts of ozone are very complex, affecting different members of the ecosystem community in different ways, and POD₁IAM_SNL is only intended to identify risks to the most sensitive vegetation (*UNECE*, 2017).

Table 1: POD_YIAM critical levels (CL) for crops (here, IAM_WH), forest trees (IAM_DF) and semi-natural vegetation (IAM_SNL), for boreal region (adapted from *UN-ECE* 2017).

Vegetation	Effect parameter	Use to assess risk of reduction in	Potential effect at CL (% reduction)	CL ^(a) (mmole O ₃ m ⁻² (PLA))	Ref10POD _Y (mmole O ₃ m ⁻² (PLA))
POD ₃ IAM_Crops	grain yield	grain yield	5%	7.9	0.1
POD ₁ IAM_DF	Total biomass	Annual growth of living biomass of trees	4%	5.7	0.6
POD ₁ CF	Whole tree biomass		2%	9.2	0.1
POD ₁ IAM_SNL	flower number	vitality of species-rich grassland	10%	6.6	0.1

Notes: (a) CL represents the ($\text{POD}_Y\text{SPEC} - \text{Ref10POD}_Y\text{-SPEC}$) required for an x% reduction.

2 Methods

2.1 The EMEP MSC-W chemical transport model

The EMEP MSC-W¹ model was used to calculate ozone concentrations and ozone uptake to vegetation for this study. The EMEP model (*Simpson et al.*, 2012, 2021) is a 3-D chemical transport model whose results underpin the integrated assessment work of LRTAP (*Amann et al.*, 2011). The performance of the EMEP model has been evaluated across a range of global sites in *Mills et al.* (2018a) and *Stadtler et al.* (2018), and evaluated and compared to a range of European regional models and observations in the CAMS_61 project ((*Fagerli et al.*, 2021a) and on web ² and for specific countries in EMEP country reports (e.g. *Klein et al.*, 2021, for Norway). The AeroVal system³ at the Norwegian Meteorological Institute also provides comprehensive information and tools concerning model performance.

For this study, version 4.44 of the model was used (*Simpson et al.*, 2021). The simulation domain extended from 30 °W to 45 °E and 30 °N to 76 °N with resolution of 0.1°×0.1° degrees latitude/longitude and 20 vertical layers from the ground to the tropopause. The lowest layer has a thickness of ca. 45m. The meteorological data required for the model are obtained from the ECMWF-IFS (European Centre for Medium Range Weather Forecasting Integrated Forecasting System) model. Initial and boundary conditions for the main gaseous and aerosol species were based on climatological observed values with prescribed trends in trans-Atlantic fluxes, while ozone levels have been corrected based on measurements at Mace Head in Ireland (*Fagerli et al.*, 2021b, section 4.2). Anthropogenic emissions come from the latest CAMS regional emissions dataset for 2017 (CAMS-REG-AP v4.2, *Kuenen et al.*, 2021).

The stomatal ozone flux and hence POD values are estimated within the EMEP model using the DO3SE (Deposition of Ozone for Stomatal Exchange) approach (*Emberson et al.*, 2000a,b, 2001; *Büker et al.*, 2012; *Simpson et al.*, 2007, 2012) for each land-cover class, and depends upon the leaf level stomatal conductance as well as a calculation of the vertical profiles of ozone down to the top of the vegetation canopy (*Tuovinen et al.*, 2009).

¹European Monitoring and Evaluation Programme, Meteorological Synthesizing Centre West

²https://aerocom-evaluation.met.no/intercomp.php?project=cams61_p2&exp=2018-rerun&par=vmro3&stats=daily#

³https://aeroval.met.no/evaluation.php?project=emep&exp_name=2021-reporting

2.2 Data assimilation system

Apart from a standard model simulation, the EMEP model can also perform simulations where observations are assimilated. The observations are used to adjust concentration fields in and around the observation location to have a better match with these (and other) observations.

In this project, the observations that are assimilated are satellite observations of NO₂ from the OMI instrument (tropospheric columns), and surface observations of NO₂ and O₃. This is different from the operational settings for the CAMS regional ensemble (Marécal *et al.*, 2015), which also assimilate SO₂, CO, and particulate matter PM_{2.5} and PM₁₀. These are assimilated in the just specified order, and only change the observed concentration fields; that is, the satellite NO₂ observations are assimilated first, and these change the NO₂ vertical profiles; then the NO₂ surface observations are analysed, and these change the NO₂ concentrations in the boundary layer; finally, the O₃ observations are assimilated, and these only change the O₃ concentrations in the boundary layer.

The assimilation is performed at the end of each hour, taking into account the observations available for that hour. After an assimilation, the model will propagate the adjusted concentrations to the next hour, and a new assimilation is performed. The concentration fields are adjusted using a 3D-var technique based on Kahnert (2008). This method is based on minimization of a cost-function that defines a penalty on the mismatch between the model simulation and the observations, and also defines a penalty on changing the concentrations. The penalty on the model-observation-mismatch includes a weighting by the observation representation error, which quantifies how much a simulation is expected to be different from an observation. This error includes contributions for the instrumental error (obtained from literature), for how representative the observation site is for the surrounding area (obtained from time-series analysis), and for the model resolution (obtained from spatial analysis). Similarly, the penalty on changing the model concentration fields includes a weighting by a background-covariance, which quantifies the allowed amplitude and spatial correlation of perturbations in the concentrations.

In the current application, the adjustment to the concentrations is computed as a 2D field of correction factors. These factors are then applied to concentrations in all model layers (for satellite data), or only below in the boundary layer (for surface observations). For NO₂ the result is that the assimilation of the satellite data results in adjustment of concentrations only in the free troposphere (above the boundary layer) in case also surface

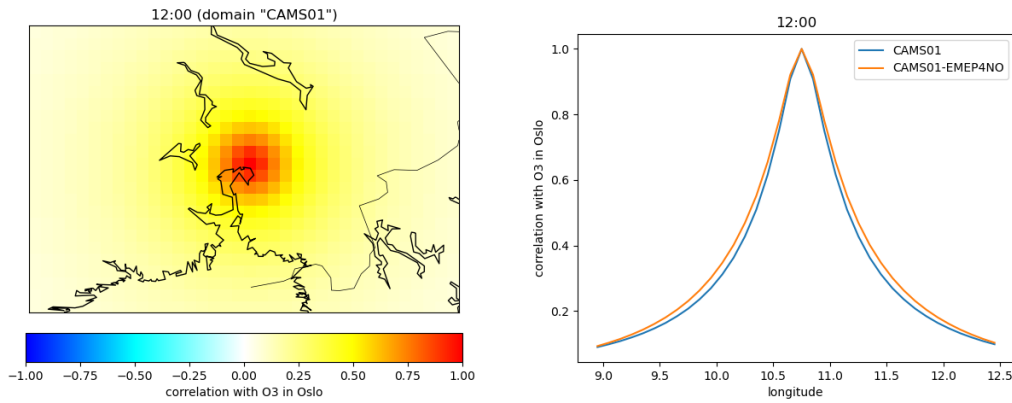


Figure 3: Left: spatial correlation between ozone changes in the grid cell over Oslo and surrounding grid cells as used in the EMEP assimilation over the European domain. Right: spatial correlation along the longitude of Oslo as used in the European domain (named "CAMS01") and the zoom over Norway (named "CAMS01-EMEP4NO")

observations are present. The background covariance for the correction fields is obtained from a statistical analysis of the difference between model simulations driven by different meteorological forecasts (NMC method, *Parrish and Derber* 1992). For a concentration change in a specific grid cell, the background-covariance defines how concentrations in surrounding grid cells are changing too. This is illustrated in the left panel of Figure 3, which shows the spatial correlation between a change in ozone concentrations over Oslo and changes in surrounding grid cells as prescribed by the covariance.

2.3 Measurements used

The analysis experiments assimilate hourly surface observations from background surface stations retrieved from the AQ e-Reporting site (*EEA*, 2021). The observations were retrieved, pre-processed and distributed by partners in the CAMS50 project for the 2018 and 2019 Validated Re-Analysis for the respective Annual air quality assessment reports (*Rouil and Meleux*, 2021).

Observations from Turkish stations were discarded as the reported time zone was inconsistent with the observations diurnal cycle. In addition one station from Kosovo showed extreme swings on the observations for mid February 2019, and was therefore excluded from the 2019 NO₂ dataset. The 2018 analysis assimilate only c.a. 90% of remaining observations. On the 2019 analysis all the remaining observations were assimilated. The analysis experiments assimilated hourly observations from 10 O₃ and 11 NO₂

Table 2: Norwegian surface stations assimilated on the 2018 and 2019 analysis.

station code	latitude °E	longitude °N	elevation m (a.s.l)	Background subclass	O ₃		NO ₂	
					2018	2019	2018	2019
NO0002R	8.2519	58.38846	200	Rural Regional	✓	✓		
NO0015R	13.90655	65.83089	440	Rural Regional	✓	✓		
NO0039R	8.87658	62.78246	210	Rural Regional	✓	✓		
NO0042R	11.88899	78.90669	290	Rural Remote	✓	✓		
NO0043R	11.52769	58.99677	180	Rural Regional	✓	✓		
NO0052R	5.20148	59.19722	30	Rural Regional	✓	✓		
NO0056R	11.07407	60.37288	280	Rural Regional	✓	✓		
NO0062A	9.48708	59.2024	25	Rural Near city	✓	✓	✓	✓
NO0063A	7.99183	58.14888	12	Urban			✓	✓
NO0065A	5.73147	58.96173	34	Suburban			✓	✓
NO0073A	10.76573	59.92295	24	Urban		✓		
NO0075A	10.46563	61.12087	212	Suburban			✓	✓
NO0081A	10.48778	59.9524	145	Rural Near city	✓	✓		
NO0088A	10.763	59.91487	100	Urban			✓	
NO0089A	10.39355	63.43038	30	Urban			✓	✓
NO0105A	10.94010	59.21020	18	Suburban			✓	✓
NO0108A	5.33245	60.46267	95	Suburban			✓	✓
NO0114A	10.5839	59.9181	62	Suburban			✓	
NO0118A	9.6219	59.13354	5	Suburban			✓	✓
NO0120A	5.31268	60.39593	35	Urban	✓	✓	✓	✓
NO0132A	10.82263	59.91411	100	Rural				✓
Total					10	11	11	10

Norwegian sites for 2018 and 11 O₃ and 10 NO₂ Norwegian sites for 2019, see Table 2 and Figure 4 for details. (Figs. S1 and Table S1 provide further information on the Nordic sites.)

Finally, we can note that in principle we would have liked to have one set of data-points for assimilation, and one for testing the results. This is done in CAMS-EMEP for Europe operationally (we divide European stations into 2/3 used in the data assimilation and 1/3 is used for validation), and we then clearly see that the results improve at the ‘independent’ stations. Unfortunately, the measurement network is so sparse in Norway (and distances so huge, even when including other Nordic sites) that we would then have a too sparse network to include in the data assimilation. Even in the operational CAMS-EMEP, all the Norwegian sites are kept due to the very limited network in Norway.

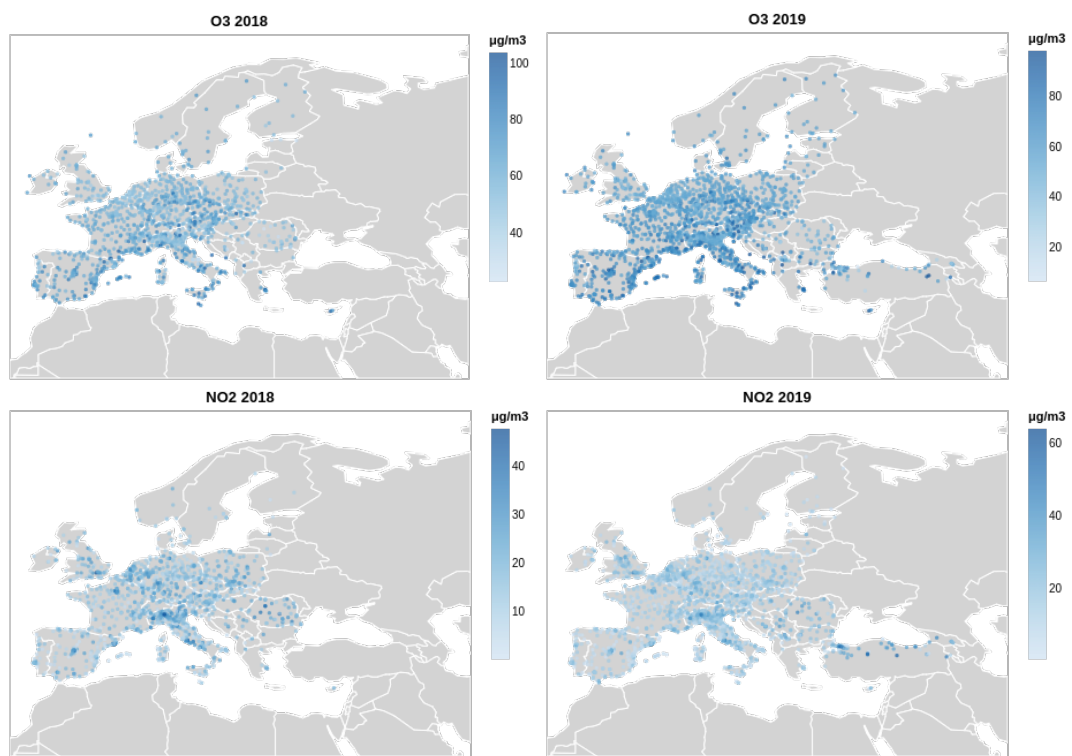


Figure 4: Surface stations assimilated in the 2018 and 2019 simulations.

3 Model evaluation

In order to generate confidence in our ability to model POD, we first have to demonstrate that the EMEP model can capture ozone concentrations over Norway to a satisfactory degree, and to demonstrate the changes brought about by the assimilation procedure. Unfortunately it is not possible to evaluate POD values in Norway (or indeed anywhere except at a few heavily instrumented sites, e.g. *Klingberg et al.* 2008; *Tuovinen et al.* 2001), but we will present comparisons with daily maximum ozone (Sects. 3.1, S1) and with EU AOT40 metrics (Sect. 3.2).

3.1 Daily maximum ozone concentrations

Figure 5 illustrates the modelled daily max. ozone and summertime diurnal variations for Birkenes in 2018, with and without the assimilation procedure. Although the base-case results (without assim.) are quite good for this site in terms of correlation ($R=0.83$) and bias (-3.5%), but many ozone peaks are under-predicted. When assimilation is used the results are much better, with $R=0.99$ and bias of just -2.6% . Further, the assimilated model captures the ozone peaks very well throughout the year.

Plots for the other Norwegian sites are given in the Supplementary, Sect. S1, and show similar improvements when assimilation is used. For example, at Tustervatn (Fig. S2) the base model misses completely the peak seen in mid-April (day 105), but this is corrected for by the assimilation scheme. Similar features can be seen for the Swedish site Esrange (Fig. S9) in 2019: this site is shown as its influence on ozone and POD values in northern Norway will become apparent in Sect. 4.

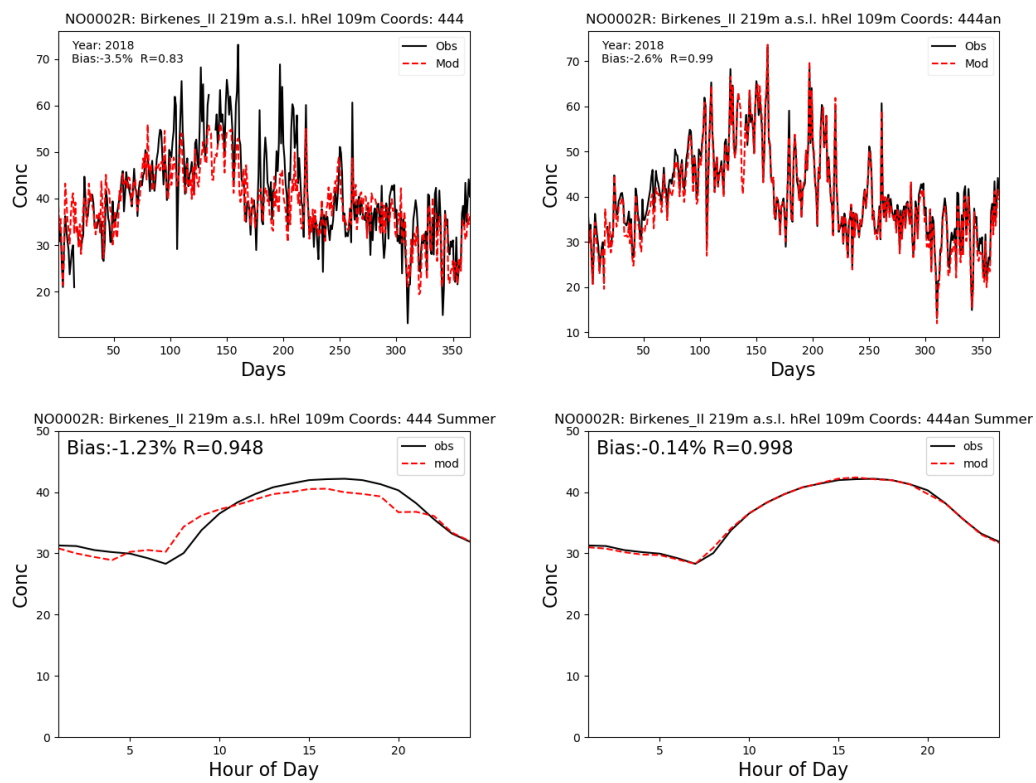
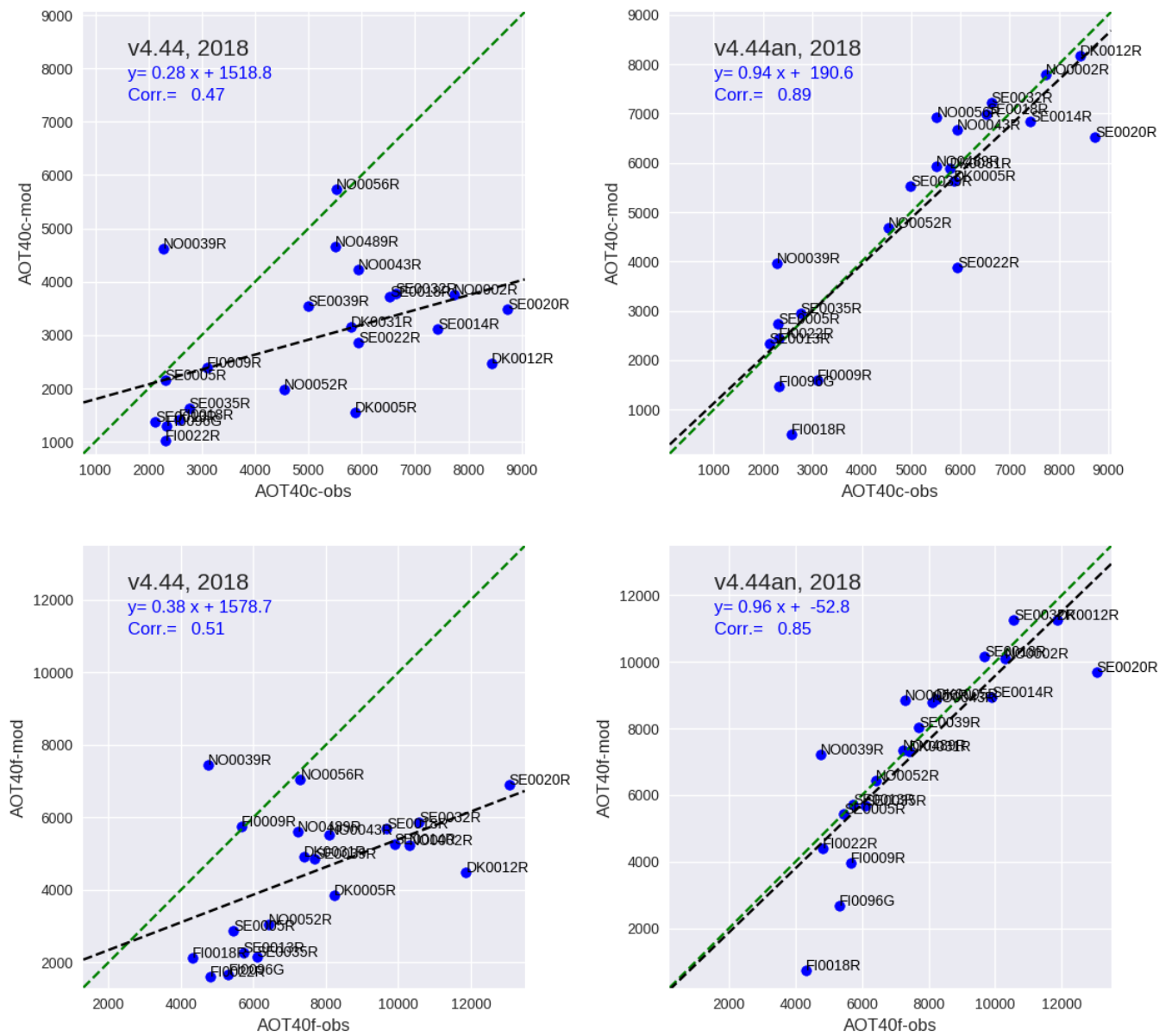


Figure 5: Comparison of modelled versus observed daily max. ozone (ppb, top), and of summertime diurnal variation (bottom). Plots on the left show base-model output, plots on the right show results when assimilation is used. Year 2018, site: Birkenes-II (NO0002R)

3.2 AOT40

As noted in Sect. 1.3 AOT40 defined via the EU approach also provides a vegetation-related metric where comparison with observations is possible. Again, it should be noted that AOT40 metrics are not expected to be very robust over Norway due to the 40 ppb threshold (*Sofiev and Tuovinen, 2001; Tuovinen, 2000*), but this comparison will serve to emphasize the usefulness of the assimilation approach.

Figures 6–7 show scatter plots of modelled versus observed AOT40 for crops and forests at all Nordic sites, both with and without assimilation. It is seen that the model performance improves dramatically when assimilation is used, both in terms of correlation and slope.



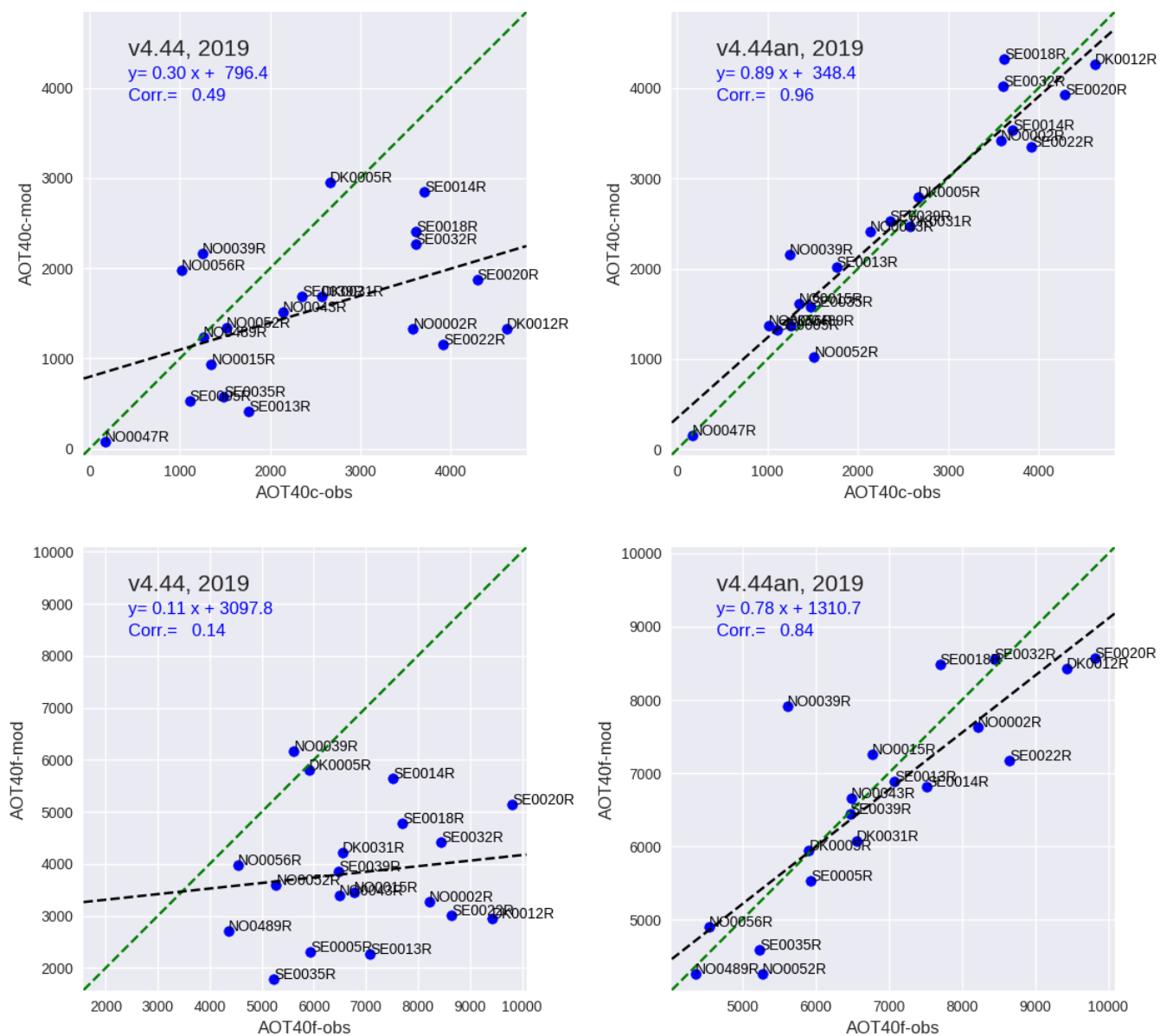


Figure 7: Modelled versus observed AOT40 at Nordic sites, as for Fig. 6, but for 2019.

4 Modelled POD values

4.1 Deciduous forests

Figure 8 shows the modelled $\text{POD}_1\text{IAM_DF}$ values for 2018 and 2019, along with changes to illustrate the impact of the assimilation procedure. In these plots the central contour line of the colour legend represents the critical level (CL, here $5.7 \text{ mmole O}_3 \text{ m}^{-2}$ (PLA)). Fig. 8(a) shows that exceedance of the CL is widespread over essentially all of Norway in both years, with values often exceeding three times CL (i.e. $17.1 \text{ mmole O}_3 \text{ m}^{-2}$ (PLA)) in south-eastern areas. Exceedances are higher in 2018, consistent with the exceptionally warm and sunny summer of that year.

Fig. 8(b) shows the changes in $\text{POD}_1\text{IAM_DF}$ caused by the assimilation procedure, this time for only the areas where deciduous forest are present in the EMEP model's land-cover. It can be seen that the assimilation procedure mainly leads to decreases of $0.1\text{--}2 \text{ mmole O}_3 \text{ m}^{-2}$ (PLA) in $\text{POD}_1\text{IAM_DF}$ over most of Norway, but increases are seen in parts of southern Norway in 2018, and close to the border with northern Sweden in 2019 (influenced by the Swedish Esrange site, c.f. Fig. S9). These plots clearly show the impact of specific sites on the assimilation changes, but as the main discrepancies between modelled and observed ozone in this study were found at the Swedish sites the changes are greater over Sweden.

A tabulation of these changes at the measurement site locations is given in Table 3. Large percentage changes are seen at Tustervatn and Kårvatn, but changes elsewhere are more modest.

4.2 Coniferous forests

Figure 9 shows the modelled POD_1CF values and changes for 2018 and 2019. Fig. 9(a) shows that exceedance of the CL for Norway spruce ($9.2 \text{ mmole O}_3 \text{ m}^{-2}$ (PLA)) is widespread over essentially all of Norway in both years, with levels of ca. $13\text{--}18 \text{ mmole O}_3 \text{ m}^{-2}$ (PLA) over most of eastern Norway. Highest levels, over $18 \text{ mmole O}_3 \text{ m}^{-2}$ (PLA), are found in southern Norway. Exceedances are somewhat higher in 2018 than in 2019. (Again, we should note that the EMEP model's CF species differs somewhat from the species suggested in the Mapping Manual (see Sect. 1.2), which will affect CL exceedance statistics to some extent. However, the differences are not expected to be major.)

Fig. 9(b) shows the changes in POD_1CF caused by the assimilation procedure, and

Table 3: Comparison of base and assimilated POD₁-IAM-DF, 2018

Code	Site	Base	Assim	$\Delta\text{POD}_1\text{IAM_DF}$ (%)
NO0002R	Birkenes II	26.01	26.11	+0.4
NO0015R	Tustervatn	11.56	10.10	-13.5
NO0039R	Kårvatn	13.39	10.36	-25.5
NO0042G	Prestebakke	25.73	25.20	-2.1
NO0043R	Svanvik	11.81	11.39	-3.6
NO0047R	Sandve	24.54	24.65	+0.5
NO0052R	Hurdal	22.66	21.20	-6.7
NO0056R	Haukenes	24.22	22.92	-5.5

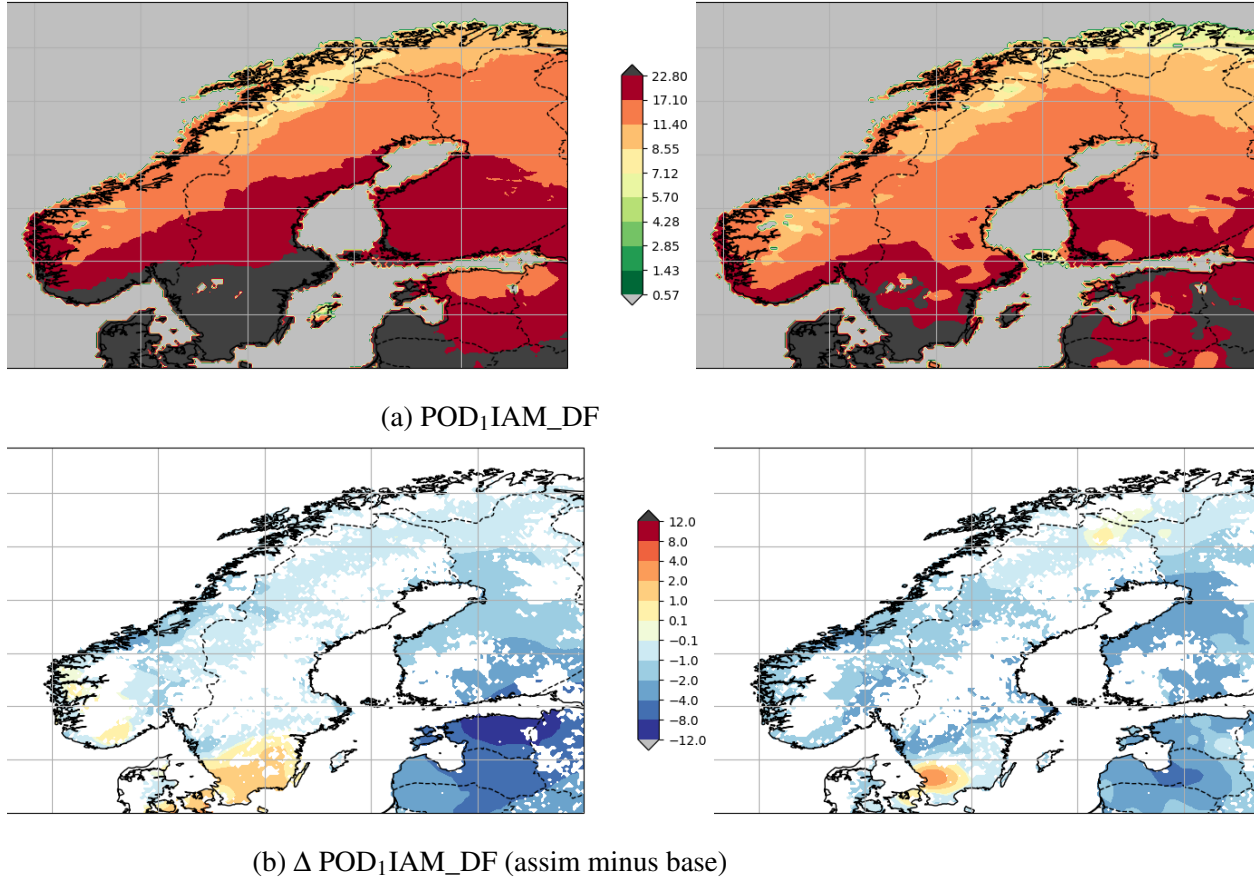


Figure 8: Modelled POD₁IAM_DF (top) for 2018 (left) and 2019 (right), and associated changes (assim minus base) in POD₁IAM_DF for areas where EMEP landcover includes deciduous trees. Units: mmole O₃ m⁻² (PLA).

Table 4: As Table 3, but for $\text{POD}_1\text{-CF}$, 2018

Code	Site	Base	Assim	$\Delta \text{POD}_1\text{CF} (\%)$
NO0002R	Birkenes II	21.16	20.78	-1.8
NO0015R	Tustervatn	0.00	0.00	-
NO0039R	Kårvatn	13.25	10.56	-22.7
NO0042G	Prestebakke	20.93	20.00	-4.5
NO0043R	Svanvik	11.03	10.70	-3.1
NO0047R	Sandve	23.97	23.80	-0.7
NO0052R	Hurdal	18.45	16.79	-9.4
NO0056R	Haukenes	19.03	17.49	-8.5

Table 5: As Table 3, but for $\text{POD}_1\text{IAM_SNL}$, 2018

Code	Site	Base	Assim	$\Delta \text{POD}_1\text{IAM_SNL} (\%)$
NO0002R	Birkenes II	9.79	10.09	+3.0
NO0015R	Tustervatn	2.79	2.42	-14.1
NO0039R	Kårvatn	2.85	2.27	-22.8
NO0042G	Prestebakke	10.05	10.06	+0.2
NO0043R	Svanvik	3.96	3.78	-4.7
NO0047R	Sandve	7.98	7.99	+0.1
NO0052R	Hurdal	8.23	7.89	-4.3
NO0056R	Haukenes	8.71	8.45	-3.0

shows similar features to those seen for $\Delta \text{POD}_1\text{IAM_DF}$. A tabulation of these changes at the measurement site locations is given in Table 4. As with $\Delta \text{POD}_1\text{IAM_DF}$, large percentage changes are seen at Kårvatn, but the changes elsewhere are more modest.

4.3 Semi-natural vegetation

Figure 10 shows the model results for $\text{POD}_1\text{IAM_SNL}$. Fig. 10(a) shows that exceedance of the CL of $6.6 \text{ mmole O}_3 \text{ m}^{-2}$ (PLA) occurs mainly in south eastern Norway. In 2019 the areas exceeding the CL are substantially smaller than in 2018. Fig. 10(b) shows the changes in $\text{POD}_1\text{IAM_DF}$ caused by the assimilation procedure, with Table 5. As with $\text{POD}_1\text{IAM_DF}$, large percentage changes are seen at Tuservatn and Kårvatn, and changes elsewhere are more modest.

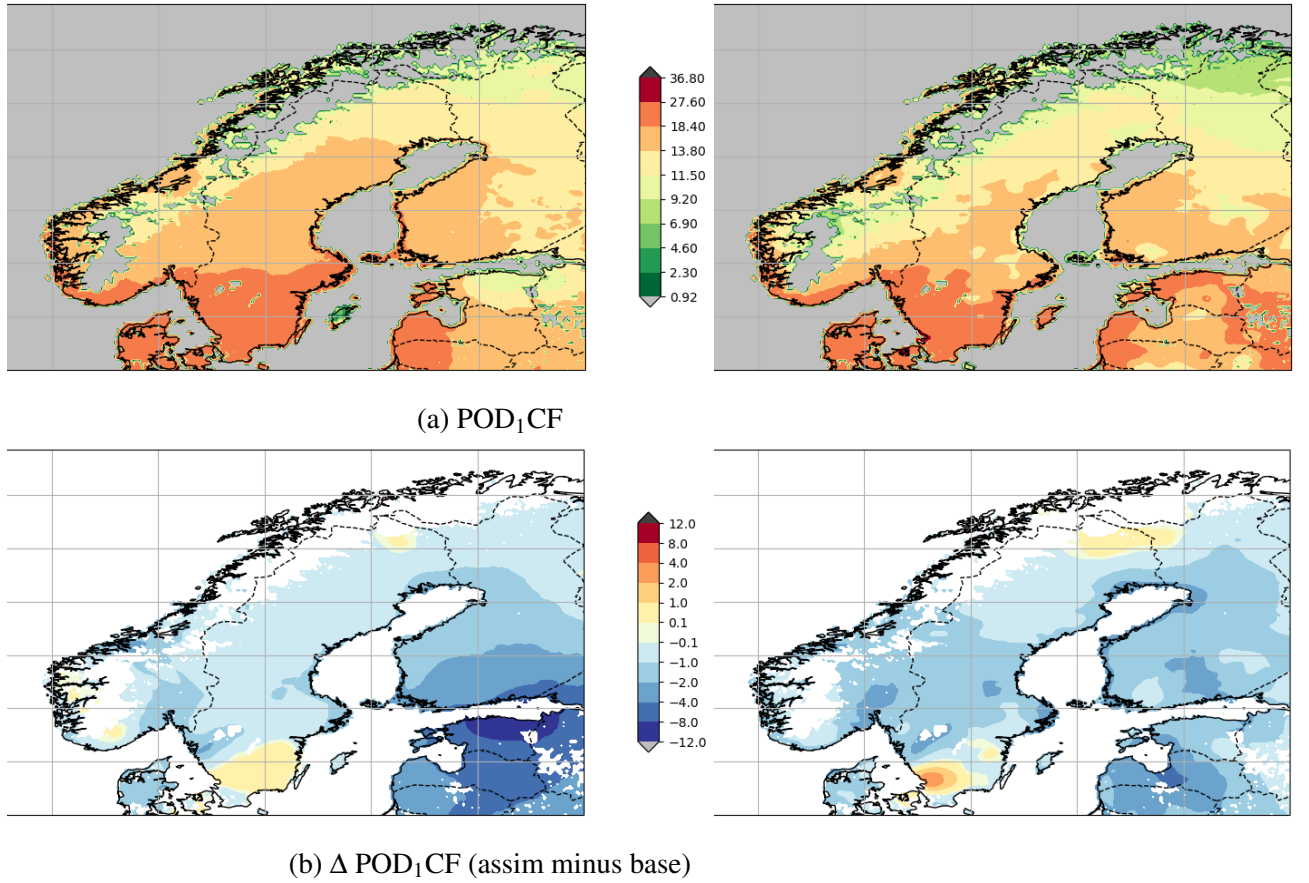
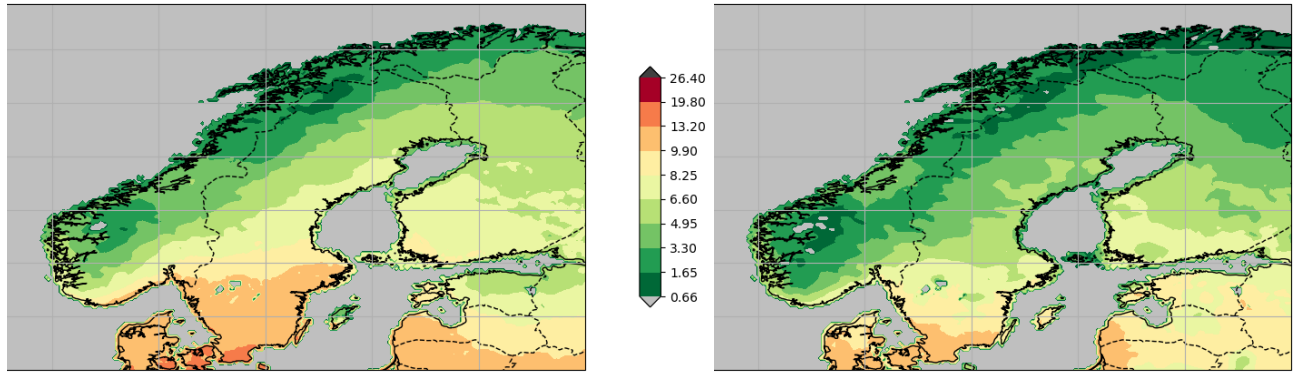
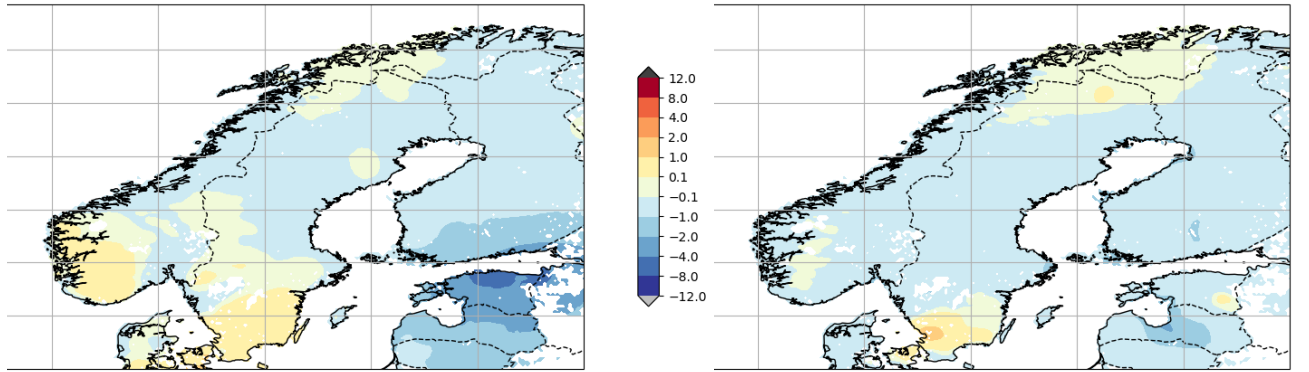


Figure 9: Modelled POD_1CF (top) for 2018 (left) and 2019 (right), and associated changes (assim minus base) in POD_1CF . Units: $mmole\ O_3\ m^{-2}\ (PLA)$.



(a) $\text{POD}_1\text{IAM_SNL}$



(b) $\Delta \text{POD}_1\text{IAM_SNL}$ (assim minus base)

Figure 10: Modelled $\text{POD}_1\text{IAM_SNL}$ (top) for 2018 (left) and 2019 (right), and associated changes (assim minus base) in $\text{POD}_1\text{IAM_SNL}$. Units: $\text{mmole O}_3 \text{ m}^{-2} \text{ (PLA)}$.

Table 6: As Table 3, but for POD₃IAM_Crops, 2018

Code	Site	Base	Assim	Δ POD ₃ IAM_Crops (%)
NO0002R	Birkenes II	19.96	22.00	+9.7
NO0015R	Tustervatn	0.00	0.00	-
NO0039R	Kårvatn	0.00	0.00	-
NO0042G	Prestebakke	20.07	21.11	+5.1
NO0043R	Svanvik	0.02	0.00	-120.1
NO0047R	Sandve	10.57	11.49	+8.4
NO0052R	Hurdal	14.67	14.01	-4.6
NO0056R	Haukenes	16.91	17.45	+3.1

4.4 Crops

Crops occupy a much smaller fraction of Norwegian land-cover than forests or semi-natural ecosystems, so here we just consider masked areas, which represent those EMEP grid cells with any crop-related land-cover. Fig. 11 shows the POD₃IAM_Crops for 2018 and 2019 for these areas. The CL of 7.9 mmole O₃ m⁻² (PLA) is exceeded along the southern and eastern coastal areas in both years, with larger exceedances in 2018.

Following *UNECE* (2017), the POD₃IAM_Crops levels may be used to make a first-order estimate yield loss for crops. If we consider a POD₃IAM_Crops values over the south-eastern coastal areas of Norway to be around 15 mmole O₃ m⁻² (PLA), and with Ref10POD_Y being 0.1 (Table 1), then Eqn. 3 becomes:

$$\Delta Y(\%) = (15 - 0.1) \times 0.64 \quad (4)$$

Or $\Delta Y \approx 10\%$. This value of yield loss is very similar to that found in many countries of the globe and indeed in southern Norway by *Mills et al.* (2018a). It should be noted that this estimate is only illustrative, and not a statement on the yield losses occurring in Norway. In order to convert the modelled POD values into more realistic effects indicators they should be combined with maps of actual vegetation cover, improved information on the phenology and crop characteristics, and information on agricultural practices with respect to crops. It is also important to note that the MM IAM_Crop species is based upon wheat, whereas in Norway many other species are economically important.

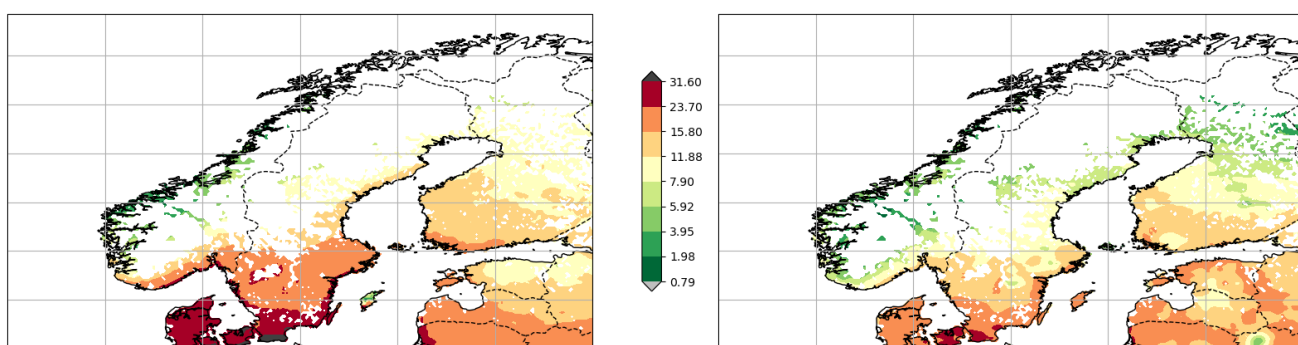


Figure 11: Modelled $\text{POD}_3\text{IAM_Crops}$ values (assimilated) for crops for 2018 (left) and 2019 (right). Areas shown have been masked to areas where the EMEP land-cover maps show crop production. As with Fig. 8, the contour levels reflect the critical levels (CL), which is $7.9 \text{ mmole O}_3 \text{ m}^{-2}$ (PLA). Contours span from 10% of the CL to $4 \times \text{CL}$ for IAM_WH.

4.5 AOT40 metrics?

Tables S2 and S3 show the base and assimilated site values of EUAOT40-Forests and MMAOT40-IAM-Crops for 2018, also with the percentage differences between ‘Base’ and ‘Assim’. These results are discussed in Sect. S2. It is readily seen that these AOT40 metrics are much more sensitive to the assimilation procedure than the POD metrics we have discussed above, mainly due to the high threshold of 40 ppb required to accumulate those metrics. Thus, despite various difficulties and issues with the POD metrics, they would seem to offer a more robust basis for mapping vegetation risks across Norway.

5 Discussion and Conclusions

For this work we have modified the EMEP MSC-W chemical transport to calculate ozone and phyto-toxic ozone doses (POD) for the years 2018 and 2019, using a 3D-Var assimilation system in order to make use of observed ozone concentrations. We have calculated POD for three indicative vegetation categories recommended by the UN-ECE Mapping Manual (MM) for large-scale modelling: IAM_DF for deciduous forests, IAM_SNL for semi-natural vegetation, and IAM_WH for crops. In addition, we include results for coniferous forests (CF) since the MM’s parameters mainly reflect Norway spruce, which is widespread in Norwegian forests. The main conclusions can be stated:

- The use of 3D-Var assimilation leads to markedly better reproduction of the daily ozone concentrations, and of the AOT40 metric (EU definition), at the Nordic sites.
- The critical levels for deciduous forests (IAM_DF) are exceeded across essentially all of Norway in both 2018 and 2019, with values often exceeding three times the CL in south-eastern areas. Exceedances are higher in 2018, consistent with the exceptionally warm and sunny summer of that year.
- For coniferous forests, exceedance of the CL for Norway spruce (which is higher than for IAM_DF) is widespread over essentially all of Norway in both years, especially in eastern and southern Norway. Exceedances are somewhat higher in 2018 than 2019.
- Exceedance of the CL for IAM_SNL occurs mainly in south eastern Norway. In 2019 the areas exceeding the CL are substantially smaller than in 2018.

- Crops occupy a much smaller fraction of Norwegian land-cover than forests or semi-natural ecosystems, so results were presented for masked areas, which represent those EMEP grid cells with any crop-related land-cover. The CL for IAM_CROPS is exceeded along the southern and eastern coastal areas in both years, with larger exceedances in 2018.
- Although we cannot give a proper estimate of yield loss for crops in Norway, the maps presented in Sect. 4.4 would allow such as estimate of the relevant agricultural maps were available. However, taking representative POD₃IAM_Crops values over the south-eastern coastal areas of Norway to be around 15 mmole O₃ m⁻² (PLA) would suggest a yield loss of about 10% for wheat. This value of yield loss is very similar to that found in many countries of the globe and indeed Europe by *Mills et al.* (2018a).
- Tests with both EU and MM definitions of AOT40 metrics were found to be much more sensitive to the assimilation procedure than the POD metrics, mainly due to the high threshold of 40 ppb required to accumulate those metrics. Thus, despite various difficulties and issues with the POD metrics, they would seem to offer a more robust basis for mapping vegetation risks across Norway.

It should be noted that there are many uncertainties associated with the calculation of POD values over Norway, which are inevitable given the rather advanced nature of the POD calculation, and the fact that Norwegian ozone levels are often close to tropospheric background levels, and thus sensitive to thresholds in metrics such as AOT40 or POD_Y when Y is as high as 3 or 6 nmole O₃ m⁻² (PLA) s⁻¹. We can note some issues which deserve further attention in future studies of this type:

Vegetation characteristics The vegetation characteristics given in the Mapping Manual, and used for the POD calculations, are generally for species in more southerly climates. This was stressed by *Falk et al.* (2021), who pointed out for example that assumed minimum, optimum, and maximum temperatures for grasslands are probably more appropriate to central than to northern Europe, and can even give unrealistically low stomatal conductances in especially perennial grasslands. Long days in Nordic summers may also impact vegetation susceptibility to ozone (*Futsaether et al.*, 2015). It seems likely that especially the growing seasons, phenology, and factors controlling stomatal conductance for vegetation in Norway differ from

those assumed in the MM. More realistic calculations of the POD levels for Norwegian vegetation will require the development of new parameterisations of the characteristics of the species of interest.

Improved land-cover In order to convert the modelled POD values into more realistic effects indicators they should be combined with maps of actual vegetation cover, improved information on the phenology as discussed above, and information on agricultural practices with respect to crops. Although the MM has a large focus on wheat, parameterisations can also be found for tomatoes and (more relevant for Norway!) potatoes.

Refined assimilation techniques

- Although the assimilation is giving very good ozone values over the measurement stations, as it should, changes are harder to verify for regions in between the stations. In principle we would have liked to have one set of data-points for assimilation, and one for testing the results. This is done in CAMS-EMEP for Europe operationally (we divide European stations into 2/3 used in the data assimilation and 1/3 is used for validation), and we then clearly see that the results improve at the ‘independent’ stations. Unfortunately, the measurement network is so sparse in Norway (and distances so huge, even when including other Nordic sites) that we would then have a too sparse network to include in the data assimilation. Even in the operational CAMS-EMEP, all the Norwegian sites are kept due to the very limited network in Norway.
- The data assimilation technique that is currently used has the disadvantage that only a single effective correlation length scale is used to distribute increments over the grid. This length scale is rather small, which is less suitable in case the observation sites are sparsely distributed such as in Scandinavia. A different technique or configuration that allows more spatial fine-tuning would be preferable.
- The data assimilation applies relative changes to the 3D ozone field based on differences between surface concentrations and observations. At night time, with low concentrations at the surface, the imposed relative changes sometimes cause large absolute changes at higher model layers. A better balancing

between absolute and relative changes is desired to avoid excessive adjustments in the boundary layer.

Finally, we can summarise that although there are many uncertain aspects of POD calculations, this study has demonstrated that the use of data assimilation leads to much improved model estimates of ozone and the more difficult AOT40 metric, which gives more confidence that the model's prediction of POD at these sites are also much improved. As noted above, predictions at locations in-between stations should also be improved, though obviously this is more uncertain. Future work would include refinements in the assimilation techniques used, especially with regard to coping with the sparse site network, but more importantly more detailed characterisation of the vegetation characteristics in this region.

Acknowledgements

Funding for this project was provided by the Norwegian Environment Agency. The computations were partly performed on resources provided by UNINETT Sigma2 - the National Infrastructure for High Performance Computing and Data Storage in Norway (grant NN2890k and NS9005k). IT infrastructure in general was available through the Norwegian Meteorological Institute (MET Norway). The CPU time granted on the supercomputers owned by MET Norway has been of crucial importance, in addition to the CPU time made available by ECMWF to generate meteorology. The work has also clearly benefited from the EMEP work funded by UNECE and the Copernicus Atmosphere Monitoring Service (CAMS) contracts, in particular the Contracts on regional forecasts and analysis (CAMS_50).

References

- Amann, M., I. Bertok, J. Borken-Kleefeld, J. Cofala, C. Heyes, L. Hoeglund-Isaksson, Z. Klimont, B. Nguyen, M. Posch, P. Rafaj, R. Sandler, W. Schoepp, F. Wagner, and W. Winiwarter (2011), Cost-effective control of air quality and greenhouse gases in europe: Modeling and policy applications, *Environmental Modelling & Software*, 26(12), 1489–1501, doi:10.1016/j.envsoft.2011.07.012.
- Büker, P., T. Morrissey, A. Briolat, R. Falk, D. Simpson, J.-P. Tuovinen, R. Alonso, S. Barth, M. Baumgarten, N. Grulke, P. E. Karlsson, J. King, F. Lagergren, R. Matyssek, A. Nunn, R. Ogaya, J. Peñuelas, L. Rhea, M. Schaub, J. Uddling, W. Werner, and L. D. Emberson (2012), DO₃SE modelling of soil moisture to determine ozone flux to forest trees, *Atmos. Chem. Physics*, 12(12), 5537–5562, doi: 10.5194/acp-12-5537-2012.
- EEA (2021), Air quality e-reporting, <https://www.eea.europa.eu/data-and-maps/data/aqereporting-9>.
- Emberson, L. (2020), Effects of ozone on agriculture, forests and grasslands, *Philosophical Transactions of the Royal Society A: Mathematical, Physical and Engineering Sciences*, 378(2183), 20190,327, doi:10.1098/rsta.2019.0327.
- Emberson, L., M. Ashmore, H. Cambridge, D. Simpson, and J. Tuovinen (2000a), Modelling stomatal ozone flux across europe, *Environ. Poll.*, 109(3), 403–413.
- Emberson, L., D. Simpson, J.-P. Tuovinen, M. Ashmore, and H. Cambridge (2000b), Towards a model of ozone deposition and stomatal uptake over Europe, *EMEP MSC-W Note 6/2000*, The Norwegian Meteorological Institute, Oslo, Norway.
- Emberson, L., M. Ashmore, D. Simpson, J.-P. Tuovinen, and H. Cambridge (2001), Modelling and mapping ozone deposition in Europe, *Water, Air and Soil Pollution*, 130, 577–582.
- EU (2008), Annex VIII. Ozone target values and long-term objectives, in *Directive 2008/50/EC OF THE EUROPEAN PARLIAMENT AND OF THE COUNCIL of 21 May 2008 on ambient air quality and cleaner air for Europe*, vol. 152, pp. L152/24–L152/25, European Union.

- Fagerli, H., H. Brenna, A. Mortier, J. Griesfeller, J. Gliss, M. Gauss, O. Jorba, S. Basart, D. Bowdalo, M. T. Pay, G. Descombes, A. Colette, B. Raux, M. Schaap, J. Tokaya, A. Segers, and R. Timmermans (2021a), Report with prioritised list of recommendations (model aspects): Analysis of results from cams_61 phase 3 - sensitivity runs, *Copernicus Report CAMS61_2019SC1_D1.3.1_202106_Prioritised_List_Recommendations_v1*, ECMWF.
- Fagerli, H., S. Tsyro, D. Simpson, Á. Nyíri, P. Wind, M. Gauss, A. Benedictow, H. Klein, Á. Valdebenito, Q. Mu, E. Grøtting Wærsted, H. Gliß, J. Brenna, A. Mortier, J. Griesfeller, W. Aas, A. Hjellbrekke, S. Solberg, K. Tørseth, K. Yttri, K. Mareckova, B. Matthews, S. Schindlbacher, B. Ullrich, R. Wankmüller, and J. Scheuschner, T. and Kuenen (2021b), Transboundary particulate matter, photo-oxidants, acidifying and eutrophying components, *EMEP MSC-W Status Report 1/2021*, The Norwegian Meteorological Institute, Oslo, Norway.
- Falk, S., A. V. Vollsnes, A. B. Eriksen, L. Emberson, C. O'Neill, F. Stordal, and T. Koren Berntsen (2021), Parameterization of the responses of subarctic European vegetation to key environmental variables for ozone risk assessment, *Biogeosc. Discuss.*, 2021, 1–37, doi:10.5194/bg-2021-260.
- Futsæther, C. M., A. V. Vollsnes, O. M. O. Kruse, U. G. Indahl, K. Kvaal, and A. E. B. Eriksen (2015), Daylength influences the response of three clover species (*Trifolium* spp.) to short-term ozone stress, *Boreal Environment Research*, 20, 90–104.
- Kahnert, M. (2008), Variational data analysis of aerosol species in a regional ctm: background error covariance constraint and aerosol optical observation operators, *Tellus B*, 60(5), 753–770, doi:10.1111/j.1600-0889.2008.00377.x.
- Karlsson, P., S. Braun, M. Broadmeadow, S. Elvira, L. Emberson, B. Gimeno, D. Le Thiec, K. Novak, E. Oksanen, M. Schaub, J. Uddling, and M. Wilkinson (2007), Risk assessments for forest trees: The performance of the ozone flux versus the AOT concepts, *Environ. Poll.*, 146(3), 608–616.
- Karlsson, P. E., H. Pleijel, and D. Simpson (2009), Ozone exposure and impacts on vegetation in the Nordic and Baltic countries, *Ambio: A Journal of the Human Environment*, 38(8), 402–405.

- Klein, H., M. Gauss, S. Tsyro, Á. Nyíri, and H. Fagerli (2021), Transboundary air pollution by sulphur, nitrogen, ozone and particulate matter in 2019. Norway, *MSC-W Data Note 1/2021*, The Norwegian Meteorological Institute, Oslo, Norway, iSSN 1890-0003.
- Klingberg, J., H. Danielsson, D. Simpson, and H. Pleijel (2008), Comparison of modelled and measured ozone concentrations and meteorology for a site in south-west Sweden: Implications for ozone uptake calculations, *Environ. Poll.*, *115*, 99–111.
- Kuenen, J., S. Dellaert, A. Visschedijk, J.-P. Jalkanen, I. Super, and H. Denier van der Gon (2021), CAMS-REG-v4: a state-of-the-art high-resolution European emission inventory for air quality modelling, *Earth System Science Data Discussions*, *2021*, 1–37, doi:10.5194/essd-2021-242.
- Langner, J., H. Alpfjord Wylde, and C. Andersson (2019), Mapping of phytotoxic ozone dose for birch, spruce, wheat and potato using the match-sweden system, *METEOROLOGI Nr 166 166*, SMHI.
- Loibl, W., W. Winiwarter, A. Kopsca, J. Zufger, and R. Baumann (1994), Estimating the spatial distribution of ozone concentrations in complex terrain, *Atmos. Environ.*, *28*(16), 2557–2566.
- Marécal, V., V.-H. Peuch, C. Andersson, S. Andersson, J. Arteta, M. Beekmann, A. Benedictow, R. Bergström, B. Bessagnet, A. Cansado, F. Chéroux, A. Colette, A. Coman, R. L. Curier, H. A. C. Denier van der Gon, A. Drouin, H. Elbern, E. Emili, R. J. Engelen, H. J. Eskes, G. Foret, E. Friese, M. Gauss, C. Giannaros, J. Guth, M. Joly, E. Jaumouillé, B. Josse, N. Kadygrov, J. W. Kaiser, K. Krajsek, J. Kuenen, U. Kumar, N. Liora, E. Lopez, L. Malherbe, I. Martinez, D. Melas, F. Meleux, L. Menut, P. Moinat, T. Morales, J. Parmentier, A. Piacentini, M. Plu, A. Poupkou, S. Queguiner, L. Robertson, L. Rouil, M. Schaap, A. Segers, M. Sofiev, L. Tarasson, M. Thomas, R. Timmermans, A. Valdebenito, P. van Velthoven, R. van Versendaal, J. Vira, and A. Ung (2015), A regional air quality forecasting system over Europe: the MACC-II daily ensemble production, *Geoscientific Model Development*, *8*(9), 2777–2813, doi: 10.5194/gmd-8-2777-2015.
- Mills, G., F. Hayes, D. Simpson, L. Emberson, D. Norris, H. Harmens, and P. Büker (2011a), Evidence of widespread effects of ozone on crops and (semi-) natural vege-

- tation in Europe (1990-2006) in relation to AOT40- and flux-based risk maps, *Global Change Biol.*, 17(1), 592–613, doi:10.1111/j.1365-2486.2010.02217.x.
- Mills, G., H. Pleijel, S. Braun, P. Büker, V. Bermejo, E. Calvo, H. Danielsson, L. Emberson, L. Grünhage, I. G. Fernández, H. Harmens, F. Hayes, P.-E. Karlsson, and D. Simpson (2011b), New stomatal flux-based critical levels for ozone effects on vegetation, *Atmos. Environ.*, 45(28), 5064 – 5068, doi:10.1016/j.atmosenv.2011.06.009.
- Mills, G., K. Sharps, D. Simpson, H. Pleijel, M. Broberg, J. Uddling, F. Jaramillo, J. Davies, William, F. Dentener, M. Berg, M. Agrawal, S. B. Agrawal, E. A. Ainsworth, P. Büker, L. Emberson, Z. Feng, H. Harmens, F. Hayes, K. Kobayashi, E. Paoletti, and R. Dingenen (2018a), Ozone pollution will compromise efforts to increase global wheat production, *Global Change Biol.*, 24, 3560–3574, doi:10.1111/gcb.14157.
- Mills, G., K. Sharps, D. Simpson, H. Pleijel, M. Frei, K. Burkey, L. Emberson, J. Uddling, M. Broberg, Z. Feng, K. Kobayashi, and M. Agrawal (2018b), Closing the global ozone yield gap: Quantification and cobenefits for multistress tolerance, *Global Change Biol.*, doi:10.1111/gcb.14381.
- Parrish, D. F., and J. C. Derber (1992), The national meteorological center’s spectral statistical-interpolation analysis system, *Monthly Weather Review*, 120(8), 1747 – 1763, doi:10.1175/1520-0493(1992)120<1747:TNMCSS>2.0.CO;2.
- Pleijel, H., H. Danielsson, L. Emberson, M. Ashmore, and G. Mills (2007), Ozone risk assessment for agricultural crops in europe: Further development of stomatal flux and flux-response relationships for european wheat and potato, *Atmos. Environ.*, 41(14), 3022–3040, doi:10.1016/j.atmosenv.2006.12.002.
- Rouïl, L., and F. Meleux (2021), Annual air quality assessment report 2018, *Copernicus Report CAMS7_2019_D1.2.1-2018_202002_2018AAR_v1*, ECMWF.
- Simpson, D., L. Emberson, M. Ashmore, and J. Tuovinen (2007), A comparison of two different approaches for mapping potential ozone damage to vegetation. a model study, *Environ. Poll.*, 146(3), 715–725, doi:10.1016/j.envpol.2006.04.013.
- Simpson, D., A. Benedictow, H. Berge, R. Bergström, L. D. Emberson, H. Fagerli, C. R. Flechard, G. D. Hayman, M. Gauss, J. E. Jonson, M. E. Jenkin, A. Nyíri, C. Richter, V. S. Semeena, S. Tsyro, J.-P. Tuovinen, A. Valdebenito, and P. Wind

- (2012), The EMEP MSC-W chemical transport model – technical description, *Atmos. Chem. Physics*, 12(16), 7825–7865, doi:10.5194/acp-12-7825-2012.
- Simpson, D., M. Gauss, Q. Mu, S. Tsyro, A. Valdebento, and P. Wind (2021), Updates to the emep/msc-w model, 2020–2021, in *Transboundary particulate matter, photo-oxidants, acidifying and eutrophying components. EMEP Status Report 1/2021*, pp. 109–121, The Norwegian Meteorological Institute, Oslo, Norway, available from www.emep.int.
- Sofiev, M., and J.-P. Tuovinen (2001), Factors determining the robustness of AOT40 and other ozone exposure indices, *Atmos. Environ.*, 35, 3521–3528.
- Stadtler, S., D. Simpson, S. Schröder, D. Taraborrelli, A. Bott, and M. Schultz (2018), Ozone impacts of gas–aerosol uptake in global chemistry-transport models, *Atmos. Chem. Physics*, 18(5), 3147–3171, doi:10.5194/acp-18-3147-2018.
- Tuovinen, J.-P. (2000), Assessing vegetation exposure to ozone: properties of the AOT40 index and modifications by deposition modelling, *Environ. Poll.*, 109, 361–372.
- Tuovinen, J.-P., D. Simpson, T. Mikkelsen, L. D. Emberson, M. R. Ashmore, M. Aurela, H. M. Cambridge, M. F. Hovmand, N. O. Jensen, T. Laurila, K. Pilegaard, and H. Ro-Poulsen (2001), Comparisons of measured and modelled ozone deposition to forests in Northern Europe, *Water, Air and Soil Pollution: Focus*, 1, 263–274, doi:10.1023/A:1013131927678.
- Tuovinen, J.-P., D. Simpson, M. Ashmore, L. Emberson, and G. Gerosa (2007), Robustness of modelled ozone exposures and doses, *Environ. Poll.*, 146, 578–586.
- Tuovinen, J.-P., L. Emberson, and D. Simpson (2009), Modelling ozone fluxes to forests for risk assessment: status and prospects, *Annals of Forest Science*, 66, 401.
- UNECE (2017), Mapping critical levels for vegetation, in *Manual for modelling and mapping critical loads and levels*, chap. 3, ICP vegetation, CEH, UK.

Supplementary material

This supplementary provides extra information on:

S1 Model evaluation - daily maximum ozone

S2 Model evaluation - daily maximum ozone

S3 Other activities - brief description of some tests on zoomed domain and topography effects conducted early in this study.

The location of the sites used for the model evaluation can be seen in Fig. S1, and further details are given in Table S1.



Figure S1: Nordic EMEP sites used in model evaluation. For links to EMEP site codes, see Table S1

Table S1: Nordic EMEP sites used in model evaluation. See also Fig. S1 for location

Code	Latitude (°N)	Longitude (°E)	Altitude (m)	Name
DK0005R	54.75	10.74	10	Keldsnor
DK0012R	55.69	12.09	3	Risoe
DK0031R	56.29	8.43	10	Ulborg
FI0009R	59.78	21.38	7	Utö
FI0018R	60.53	27.67	4	Virolahti III
FI0022R	66.32	29.40	310	Oulanka
FI0037R	62.58	24.18	180	Ähtäri II
FI0096G	67.97	24.12	565	Pallas (Sammaltunturi)
NO0002R	58.39	8.25	219	Birkenes II
NO0015R	65.83	13.92	439	Tustervatn
NO0039R	62.78	8.88	210	Kårvatn
NO0042G	78.91	11.89	474	Zeppelin mountain (Ny-Ålesund)
NO0043R	59.00	11.53	160	Prestebakke
NO0047R	69.45	30.03	30	Svanvik
NO0052R	59.20	5.20	15	Sandve
NO0056R	60.37	11.08	300	Hurdal
NO0489R	59.20	9.52	20	Haukenes
SE0005R	63.85	15.33	404	Bredkälen
SE0011R	56.017	13.15	175	Vavihill
SE0012R	58.80	17.38	20	Aspvreten
SE0013R	67.88	21.07	475	Esrang
SE0014R	57.39	11.91	5	Råö
SE0018R	57.16	14.78	180	Asa
SE0019R	57.95	12.40	65	Östad
SE0020R	56.04	13.15	190	Hallahus
SE0022R	60.09	17.51	45	Norunda Stenen
SE0032R	57.82	15.57	261	Norra-Kvill
SE0035R	64.25	19.77	225	Vindeln
SE0039R	59.73	15.47	132	Grimsö

S1 Model evaluation - daily maximum ozone

Fig. 5 showed modelled versus observed daily max. ozone and diurnal ozone patterns for Birkenes for 2018, for model versions with and without assimilation. Here we give corresponding results for the other Norwegian sites, and also for the Swedish site Estrate in 2019.

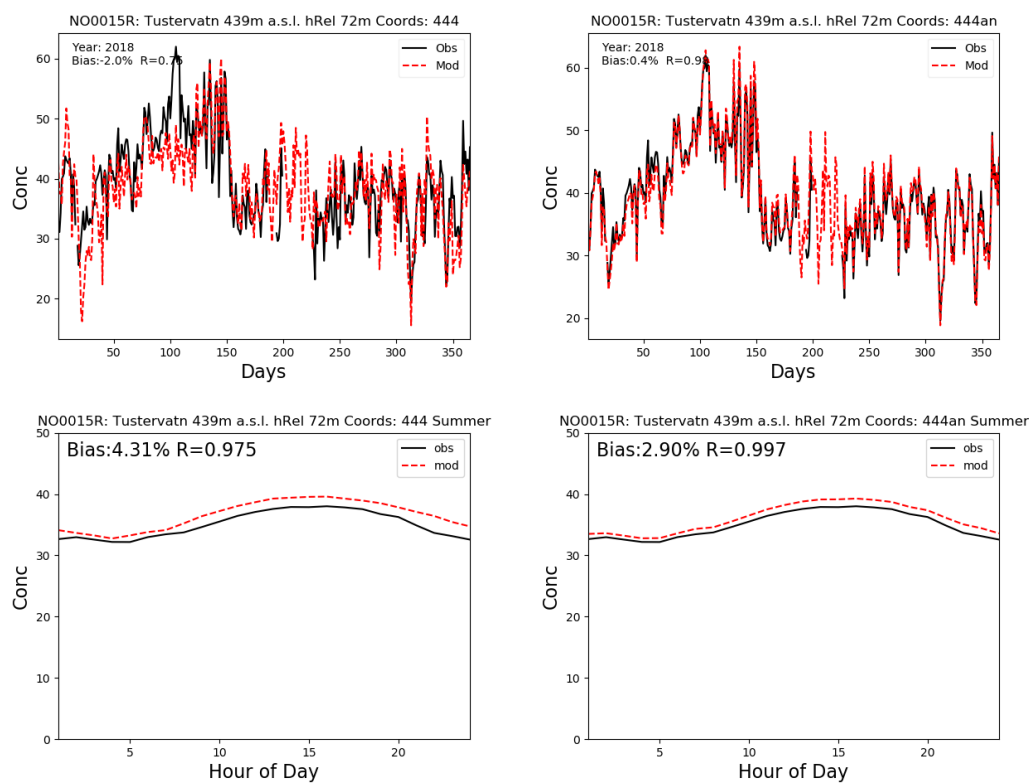


Figure S2: Comparison of modelled versus observed daily max. ozone (ppb, top), and of summertime diurnal variation (bottom). Plots on the left show base-model output, plots on the right show results when assimilation is used. site: Tustervatn (NO0015R), Year: 2018

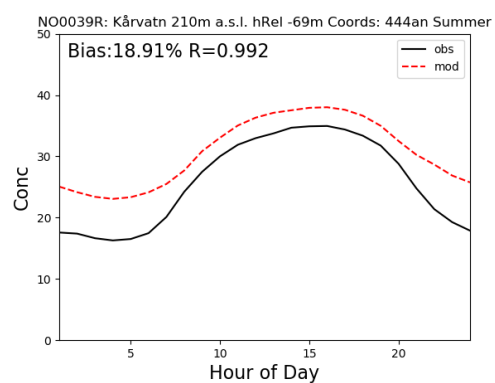
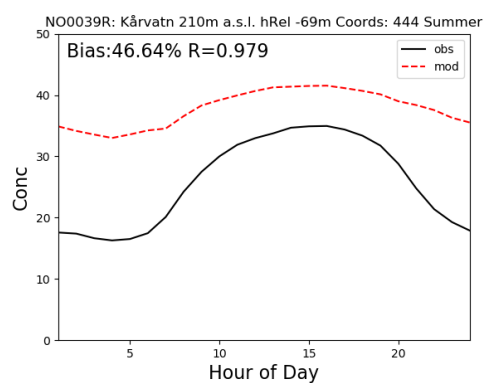
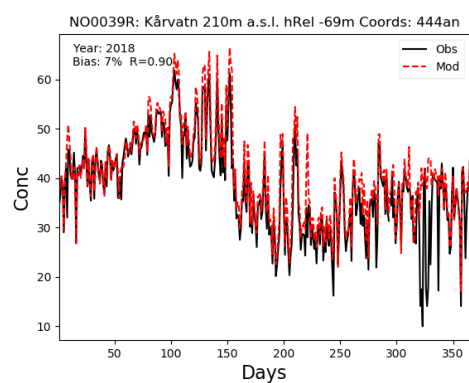
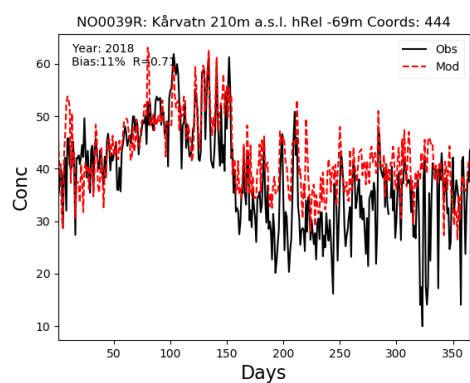


Figure S3: As Fig. S2, but for site: Kårvatn (NO0039R), Year: 2018

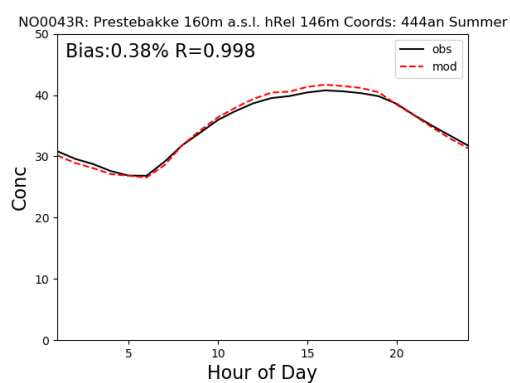
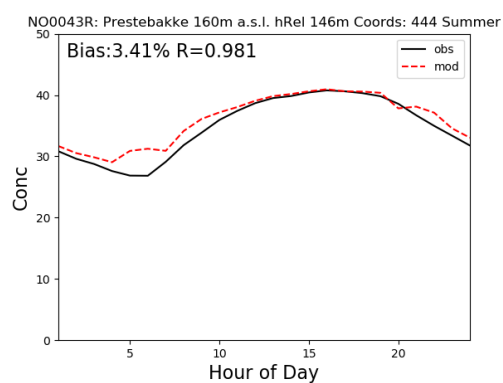
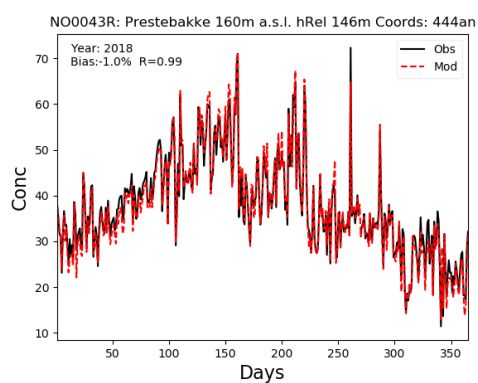
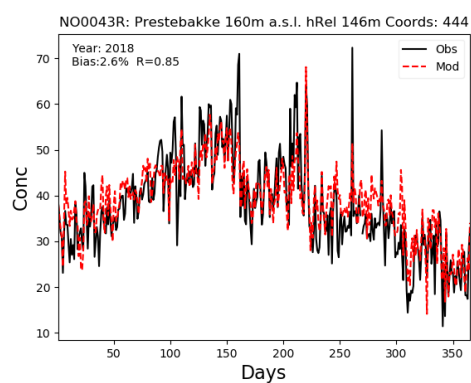


Figure S4: As Fig. S2, but for site: Prestebakke (NO0043R), Year: 2018

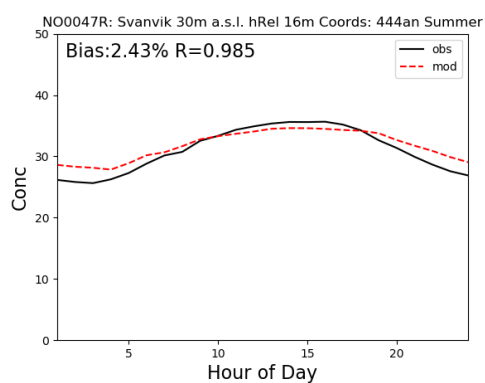
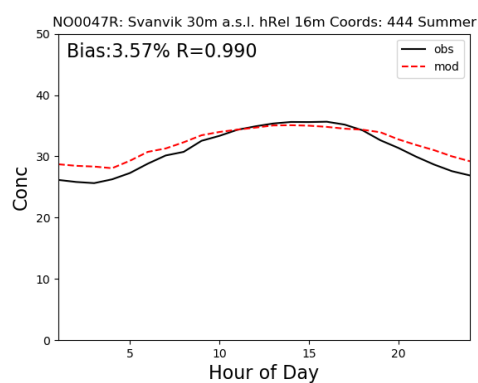
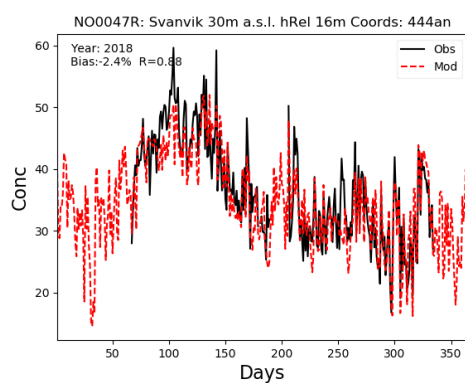
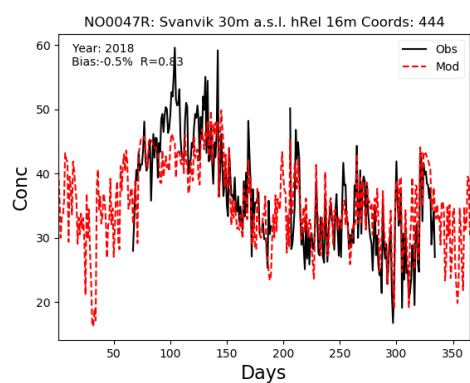


Figure S5: As Fig. S2, but for site: Svanvik (NO0047R), Year: 2018

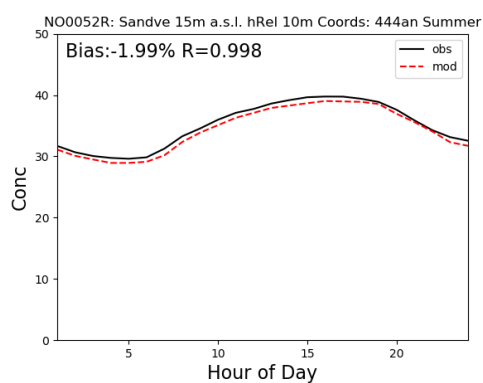
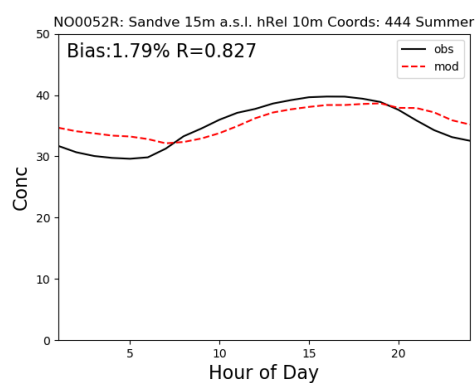
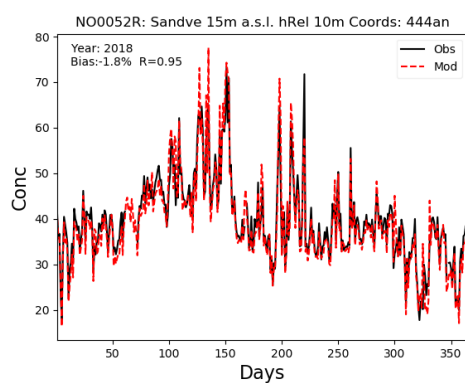
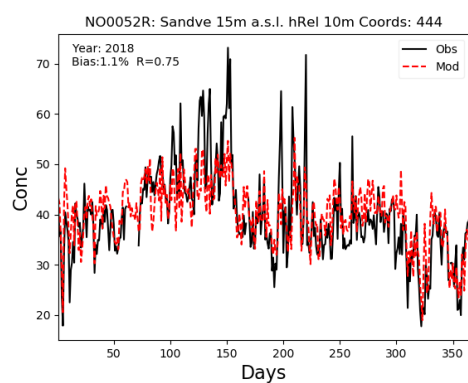


Figure S6: As Fig. S2, but for site: Sandve (NO0052R), Year: 2018

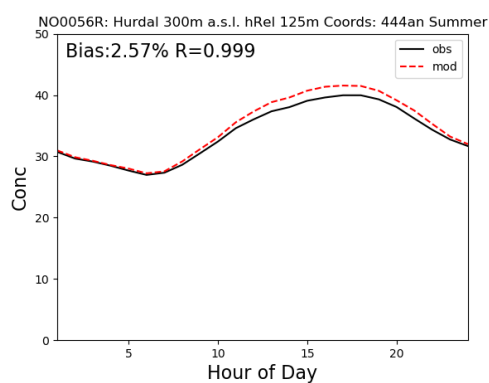
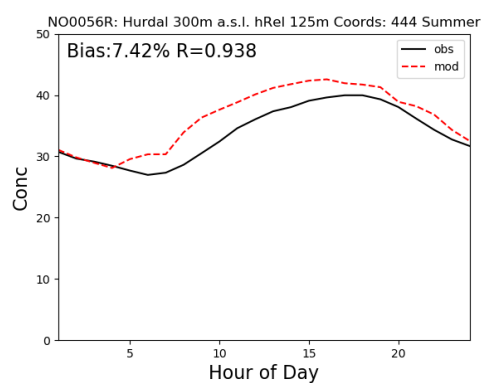
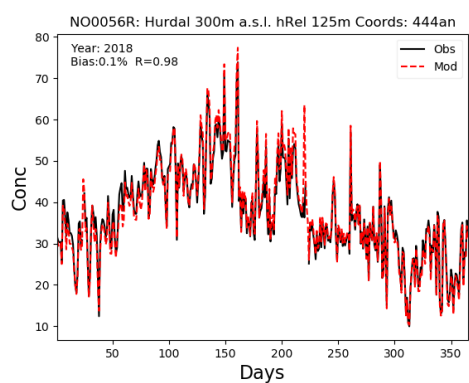
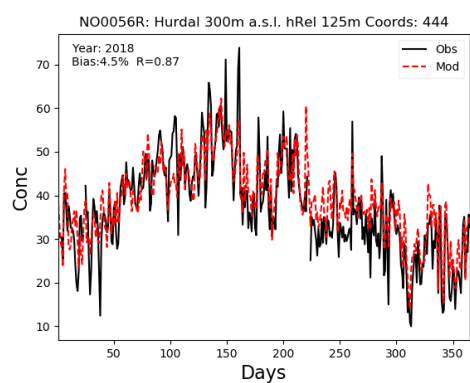


Figure S7: As Fig. S2, but for site: Hurdal (NO0056R), Year: 2018

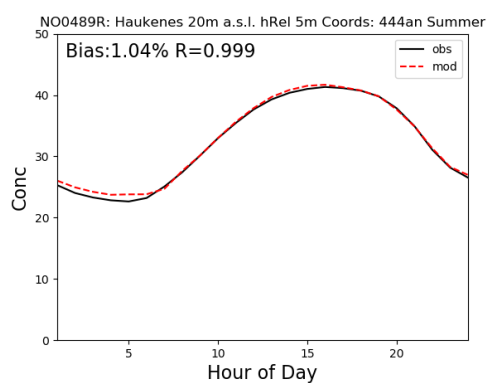
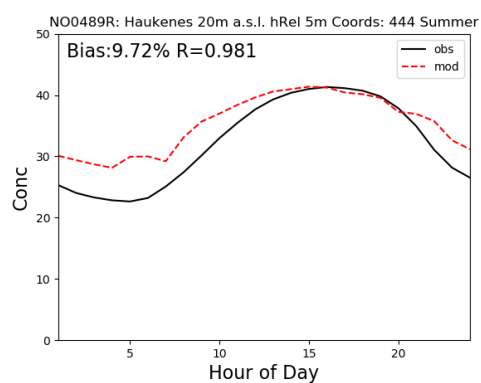
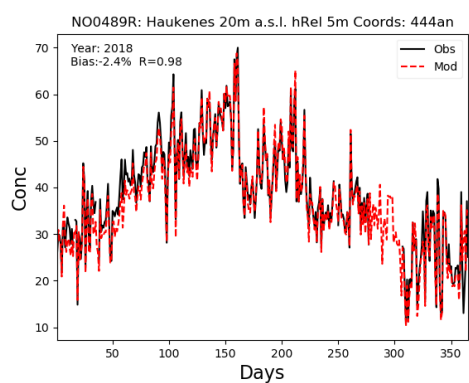
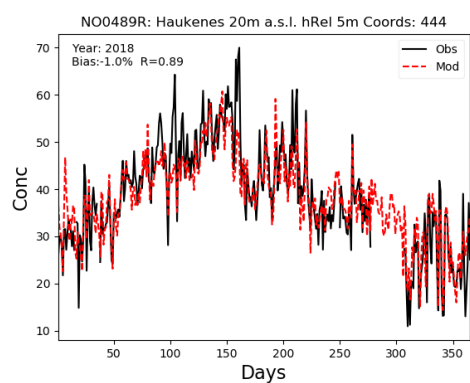


Figure S8: As Fig. S2, but for site: Haukenes (NO0489R), Year: 2018

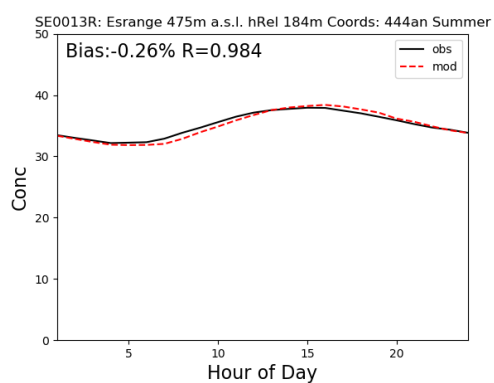
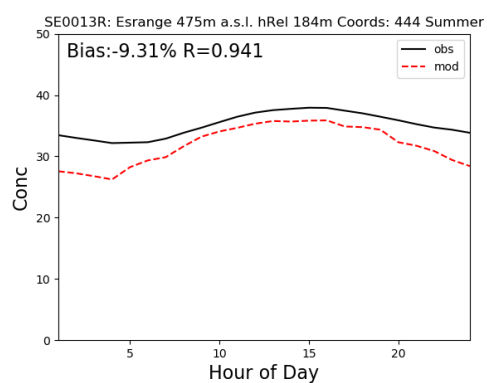
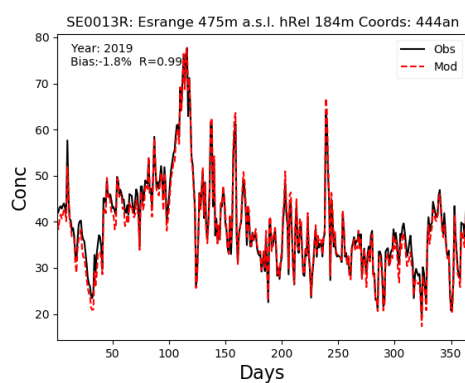
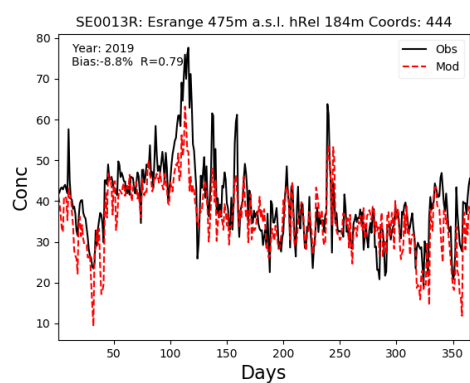


Figure S9: As Fig. S2, but for Swedish site: Estringe (SE0013R), Year: 2019

S2 Impacts on AOT40 metrics

Although the focus of this report has been on POD_Y , as it is the metric thought to best represent risk to vegetation, it is instructive to illustrate the impact of assimilation on the modelled AOT40 values. Here we illustrate one case each for the EU and Mapping Manual MM) definitions of AOT40 (see Sect. 1.1).

Tables S2–S3 provide the base and assimilated model estimates, corresponding to results shown for POD in Tables 3–6. Considering first Table S2, it is clear that assimilation can have dramatic effects on the estimated EUAOT40 values, with increases of ca. 30–40% at some sites. With the exception of Kårvatn, these changes are substantially more than those seen for POD_Y in Table 3. The MMAOT40 results for crops shown in Table S3 are even more dramatic. Use of assimilation can increase estimated MMAOT40 by up to 150%, with the smallest non-zero change 54%.

The greater sensitivity of AOT compared to POD is readily explained by two important factors:

1. The threshold of 40 ppb needed to accumulate AOT40 is close to, or often above, ozone levels experienced in Norway. Thus, on many occasions, significant AOT40 accumulation cannot take place. With POD, on the other hand, even ozone levels as low as 20 ppb can contribute to ozone fluxes and POD_Y accumulation (*Tuovinen et al.*, 2007).
2. As discussed in Sect. 1.1, the MMAOT40 metric uses O_3 concentrations from canopy height, and not directly from observations (which are usually at 2–3 m height). For crops the assumed canopy height is 1 m, and O_3 concentrations at that height can be significantly lower than those measured (or modelled) for e.g. 3 m height. This extra reduction in O_3 makes exceedance of the 40 ppb threshold even harder than with EUAOT40, and the results are correspondingly more sensitive to changes in estimated ceO_3 concentration.

Table S2: Comparison of base and assimilated EUAOT40-Forests, 2018

Code	Site	Base	Assim	Δ (%)
NO0002R	Birkenes II	8585.50	11411.97	+28.3
NO0015R	Tustervatn	5045.82	6708.86	+28.3
NO0039R	Kårvatn	8811.31	8223.59	-6.9
NO0042G	Prestebakke	9913.91	12178.10	+20.5
NO0043R	Svanvik	1811.31	2427.48	+29.1
NO0047R	Sandve	5868.05	8844.49	+40.5
NO0052R	Hurdal	10266.21	10527.02	+2.5
NO0056R	Haukenes	9462.69	10500.38	+10.4

Table S3: Comparison of base and assimilated MMAOT40-IAM-CROP, 2018

Code	Site	Base	Assim	Δ (%)
NO0002R	Birkenes II	92.06	573.52	+144.7
NO0015R	Tustervatn	2.73	4.73	+53.9
NO0039R	Kårvatn	68.37	35.42	-63.5
NO0042G	Prestebakke	62.05	442.42	+150.8
NO0043R	Svanvik	0.00	0.00	-
NO0047R	Sandve	258.00	1134.76	+125.9
NO0052R	Hurdal	85.95	243.73	+95.7
NO0056R	Haukenes	34.01	186.77	+138.4

S3 Other activities

Here we briefly mention two sets of tests which were conducted, but which were not found to lead to any improvement in the EMEP model performance for this study: (i) use of zoomed domain over Norway (Sect. S3.1), and (ii) use of topographic correction to the site outputs (Sect.S3.2). (They are mentioned here for the sake of completeness in terms of project activities.)

S3.1 Experiments with zoom over Scandinavia

The method used to parameterize the covariance (see section 2.2) has the advantage that it is computationally efficient in the assimilation, but it has the disadvantage that it effectively defines the same correlation structure for the entire domain. This structure is an average over the domain used in the NMC simulations with different meteorology that define the covariance, which is by default the entire European domain of the EMEP model.

It has been evaluated how the correlation structure changes if a smaller domain would be used, in this case a domain focusing on the target area for this project. The right panel of Fig. 3 shows that this effect is rather small: the spatial correlation calculated over a domain covering only Norway is somewhat stronger than that calculated over the full domain, but the difference is small.

The new background covariance has been used in a simulation and assimilation runs in zooming mode, where the model is configured to run on the smaller domain, reading boundary conditions that were saved from the runs over Europe. The computation costs of such a run are much smaller due to the smaller number of simulated grid cells. Comparison of the results between the zoomed simulation and the European run revealed only small differences, indicating that to simulate ozone over Norway it might be sufficient to use a smaller domain enclosing the country. Likewise, the assimilation results are very similar too, since also the covariance structures hardly differed.

S3.2 Topographic correction

Typically, ozone concentrations from the EMEP model are extracted from the model's lowest layer, which has a thickness of ca. 45 m. The model coordinate system is, however, terrain following, so that the altitude of 'ground' level follows the $0.1^\circ \times 0.1^\circ$ topog-

raphy varies from grid-to-grid. The measurement sites used in this report have a range of altitudes, e.g. from 5 m to 440 m for the Norwegian sites (Table 2), and so it could be anticipated that it would be better to extract O_3 from some upper layers from the model, in order to best simulate observed levels and diurnal patterns. Although this is not really practical for the 2-D hourly fields used for mapping, such an extraction is possible for specific sites in the EMEP model. For this project we tested extraction of data from higher altitude levels based upon either a simple comparison of site-altitude with the model's local ground-level altitude, or against a 'relative altitude' which is derived by comparing the site-altitude with local terrain (similar to the method used by *Loibl et al.* 1994). Neither method resulted in improved model-measurement comparisons, which suggests that the model's default terrain-following system works well for the Norwegian stations.